SEP. - DEC. 2021 • Volume XXII Number

THE ASEAN JOURNAL OF RADIOLOGY

Highlight

- Original Article
- Case Report
- ASEAN Movement in Radiology

Official Journal of
The Royal College of Radiologists of Thailand,
ASEAN Association of Radiology, and
Foundation for Orphan and Rare Lung Disease

ISSN 2672-9393

The ASEAN
Journal of Radiology

CONTENTS

THE ASEAN JOURNAL OF RADIOLOGY
ISSN 2672-9393

From The Editor

Received 23 December 2021 ; accepted 23 December 2021
doi:10.46475/aseanjr.v22i3.160

Thailand has passed the COVID-19 crisis, and is facing a new challenge

It is October that the average of COVID-19 infection rate is lower to less than 10, 000 cases a day in Thailand after rocket-shooting to more than 20,000 cases a day in August, killing hundreds of people and 4 doctors, 2 of whom are radiologists. The decreasing rate persists to less than 5,000 cases a day in December and lives seem to return to normal in all parts of Thailand. The Royal College of Radiologists of Thailand (RCRT), in corporation with the Foundation for Orphan and Rare Lung Disease (FORLD), welcomed onsite participants in a hybrid-conference on high resolution computed tomography (HRCT) for the first time in this year, during 4-5 December 2021 in Bangkok, after cancellation of the hybrid 2021 annual meeting in March and monthly online activities were promoted instead. From the mentioned conference, the results from the discussions in the multidisciplinary working group for interstitial lung disease focusing on estimation of disease and fibrosis on HRCT are summarized in this issue.

A hybrid conference on HRCT in Bangkok during 4-5 December 2021, held by RCRT and FORLD.

And then the second hybrid radiological conference was the annual meeting of the Thai Society of Radiological Technologists (TSRT), during 19-21 December 2021, in Bangkok. To prepare for the International Society of Radiographers and Radiological Technologists (ISRRT) Word Congress which will be held in Bangkok in 2022, TSRT selected its best society ambassadors, namely, Miss Radiology Queens, in its onsite gala dinner, apart from 3 full days of academic activities.

Miss Radiology Queen and the editor at the Gala of the TSRT annual meeting.

RadioVolunteer, the teleradiology project run by radiologist volunteers, RCRT and J.F Advance Med Co, Ltd. [2], ended on 25 December 2021 after the interpretation of more than 280,000 chest radiographs for infected patients in 143 prisons across Thailand, several communities and field hospitals in Bangkok, and provinces in other parts of Thailand since 2 June 2021, a few weeks before the peak infection rate in August. It is believed that RadioVolunteer was a significant factor that saved the infected prisoners, reducing the case fatality ratio to approximately 0.12%, comparing to 0.98% in communities [1].

Mrs. Nipha Ngamtrairai, the director of prisons in Songkla, a province in the deep south of Thailand (left), the editor (middle), and Mr. Adisorn Taprig (right) at one of the participating prisons, representing government, non-profit and private sectors, in the RadioVolunteer project.

RadioVolunteer in a prison (left) and a community (above).

Sixty-three tourists infected with the highly concerned Omicron variant of COVID-19 has been found in Thailand since 1 December. To balance between the economic contribution from tourism which accounted for around 20% of the gross domestic product (GDP) in 2019 [3], significantly higher than most other countries, and the prevention of another crisis from this fatal virus, the government is trying its best to find the epitome for the country.

Wiwatana Tanomkiat, M.D.
Editor,
The ASEAN Journal of Radiology
Email: aseanjournalradiology@gmail.com

THE ASEAN JOURNAL OF RADIOLOGY
ISSN 2672-9393

References

1. Coronavirus disease 2019 Epidemic Administration Center, Ministry of the Interior (MCU) [Internet]. Bangkok: MCU; 2020 [cited 2021 Dec 23]. [COVID 19: Thailand situation]. Available from: https://www.moicovid.com/23/12/2021/uncategorized/5947/. Thai.

2. Tanomkiat W, Taprig A, Piyavisetpat N. RadioVolunteer, a novel combination of social, management and technological innovations by the Royal College of Radiologists of Thailand in response to the COVID-19 pandemic. ASEAN J Radiol [Internet]. 2021 [cited 2021Dec.27]; 22(2): 57-66. Available from: https://www.asean-journal-radiology.org/index.php/ajr/article/view/146.

3. Theparat C. Prayut: zones vital for growth. Bangkok Post [Internet]. 2019 Sep 19 [cited 2021 Dec 26]; Sect: Business. Available from: https://www.bangkokpost.com/business/1753349/prayut-zones-vital-for-growth.

Original Article

Quantitative CT characterization of normal lung anatomy: In relation to locations and gender and study of various lung volume estimation

Hon Keong Chang, M.B.B.S. (IMU), M. Med (Radiology) [1] [2]
Shahizon Azura Mohamed Mukari, MBChB (Glasgow), M. Med (Radiology) [1]
Nik Azuan Nik Ismail, MBBCH BAO (IRELAND), M. Med (Radiology) [1]
From [1] Department of Radiology, Faculty of Medicine, Universiti Kebangsaan Malaysia Medical Center, Kuala Lumpur, Malaysia.
[2] Department of Radiology, Hospital Sultanah Bahiyah, Kedah Darul Aman, Malaysia.
Address correspondence to Shahizon A.M.M (e-mail: shahizon@ppukm.ukm.edu.my) and H.K. Chang (e-mail: honkeong28@gmail.com)

Received 17 December 2020; revised 26 October 2021; accepted 27 November 2021
doi:10.46475/aseanjr.v22i3.100

Abstract

Background: Mean lung parenchymal attenuation (MLA) may show gender differences and vary in different locations. Lung volume estimations play an important role in lung transplantation workout. In the current study, we focus on quantitative measurement of lung volume using different estimations obtained through calculated formulae from CT images and Chest Radiograph. This study could help to generate data for future references, particularly for Malaysia or Southeast Asia.

Objective: To study the MLA in relation to the location, patient's position and gender differences, in order to find the correlation of various lung volume estimation methods.

THE ASEAN JOURNAL OF RADIOLOGY
ISSN 2672-9393

Materials and Methods: This was a retrospective cross-sectional study. A total of 62 patients' CT images were selected and measurements of MLA were analyzed at lung apex, main carinal level (MCL), and base level (BL). At MCL and BL, the MLA was measured in three regions which were anterior, middle and posterior regions. A total lung volume of 26 from the 62 study subjects was also estimated using the predictive equation (method i), estimation from the frontal chest radiograph (method ii), ellipsoid formula using measurement from CT images (method iii) and semi auto-segmentation and volumetric calculation (method iv).

Results: MLA of the right lungs range from -860±9.52 to -787.66±14.8 HU. MLA of the left lungs range from -845.60±10.0 to -789.66±14.0 HU. MLA at middle MCL is lower than apex and middle BL bilaterally ($p<0.05$). Male subjects have lower lung attenuation with several areas showing a statistically significant difference ($p<0.05$). The four lung volume estimations show moderate to strong linear correlation ($r = 0.565 – 0.899$).

Conclusion: Variation of MLA among MCL, apex and BL could be related to better chest expansion at MCL. The posterior part of the lungs shows a higher value of MLA and this is related to the supine position during scanning that results in a lesser degree of chest expansion at the posterior part and gravity influence. Lung volume estimation is possible using demographic data, a chest radiograph or the ellipsoid formula.

Keywords: Mean lung attenuation, Lung volume estimation, Ellipsoid formula.

Introduction

Computed Tomography (CT) scan is an important imaging modality that provides cross-sectional images with three-dimensional reconstruction [1,2]. Images are presented as a range of grayscale and can be calculated in Hounsfield Units (HU), using density number of water as the main reference "0" [1]. In other words, structures with density higher than water will be presented as a positive HU; whereas structures with lower density will be presented as a negative HU, such as lung parenchyma and adipose tissue [1].

In 2016, Stein et al. conducted an analysis on 42 CT images of a paediatrics age group and it was found that lung attenuation was in a rapid reducing trend among growing children younger than 2 years old, as the lung volume was growing larger [3]. Lung attenuation was also higher in the dependent part of the lung, related to gravity [3]. The attenuation value of a normal lung may show variation due to gender and age factors according to previous studies; however, in a cohort study by Zach et al., there was no persistent association demonstrable between lung attenuation and the age group or the gender factor on his multivariate analysis [4]. In another study by Smit HJM et. al, no significant difference in lung attenuation measurement between male and female was revealed [5]. Lung attenuation was found to be lower at the main carina level compared to the top, but the value increased upon expiration [5]. According to another study on 155 adults patients by Kauczor et. at, the mean lung density (MLD) measured -813 HU during full inspiration and it increased to -736 HU during expiration [6]. Therefore, the inspiratory effort of subjects during CT acquisition may be one of the factors affecting the mean attenuation value of the lung parenchyma.

Besides, the lung volume could be measured from CT images, using manual contour delineation or automatic lung segmentation [2]. However, CT lung volumetry was still not the gold standard in total lung volume estimations and it also exposed patients with radiation [2]. From 1930's, there were a few studies focusing on the estimation of the lung volume or lung capacity based on chest radiographs, namely the study conducted by Hurtado and Fray in 1933 [7-8],

Barnhard et al. [7 - 8], Gamsu et al. [7], Reger et al. [8] and others. These studies published data and estimations of the total lung volume from chest radiographs, correlating with plethysmography [7-8]. One of the methods published in some of these studies utilized ellipsoid formulas [7-8].

Another method published by Canal et al., assessed the estimations from the measurement based on a frontal chest radiograph of small mammals [9]. The estimation equation is $V^*_L = 0.496 \,.\, V_{RX.}$; whereby V_{RX} is the measurement of the volume containing lungs and mediastinum and

$$V_{RX} = W \,.\, \frac{(H_1 + H_2)}{2} \,.\, \frac{(w_1 + w_2)}{2}$$

. W is the straight line width between two costophrenic recesses; H_1 is the height from W to the top of the left lung; H_2 is the height from W to the top of the right lung; w_1 is the left lung width at the midpoint of the diaphragm dome; w_2 is the right lung width at the midpoint of the diaphragm dome (Figure 1). This formula shows a possible similarity or correlation to the previously published calculations, where it could be correlated with ellipsoid formula: Volume, V = 0.523 . a . b . c ; whereby a, b and c are the diameters of the ellipsoid [9].

Furthermore, there are also equations for the predicted lung volume suggested by Konheim et al.: Predicted TLV (pTLV) = [-630.819 + (967.100*Gender) + (25.197*Height) - (713.838*Race) + (15.103*Age)]/1000; Gender: Male (1), Female (0); Race: African American (1), others (0); Height in cm, Age in years. This formula was created by correlating with 4 different variables and CT volumetry calculation of 400 patients using lasso regression, which was further tested with one of the gold standard – body plethysmography and lung function test. This predictive equation also shows a strong positive correlation between the predicted total lung volume and the total lung capacity ($r = 0.82$; $p<0.0001$; 95% CI, 0.59 – 0.93) [10].

The total lung volume estimation plays an important role in the clinical procedure as well as in research fields [7]. It is important particularly in lung transplantation workout and size-matching of the lung volume for donors and

recipients [7 & 10]. This study utilized 4 different methods of quantitative measurement to estimate the total lung volume of Malaysian adults; i.e. based on the predictive equation published by Konheim (method i), based on estimation from the frontal radiograph published by Canals M (method ii), the Ellipsoid formula (method iii) and semi auto-segmentation and volumetric calculation using DICOM compatible program, Osirix Lite (method iv). Furthermore, the correlations between these four methods were looked into.

CT scan examination imposed more radiation to the patient compared to a chest radiograph. For lung transplantation patients, they may not need to undergo CT scan examination in order to estimate their lung volume, if method i and ii showed a positive correlation with the other described methods. Method i requires the patient's demographic data [10], whereas method ii needs calculation from a frontal chest radiograph [9], which is easily available [1]. Method i is considered as good as the gold standard as it shows the correlation with body plethysmography and the lung function test.

This study aims to generate local data for a mean lung volume and lung parenchymal attenuation (MLA) for Malaysian adults, which could become the reference for future studies and in clinical settings in Malaysia and perhaps in Southeast Asia. In clinical practices, the area of low lung attenuatiuon (LAA%) is used to assess the extent of emphysema, whereas the high attenuation area (HAA%) assesses the extent of lung infections, interstitial lung diseases and ARDS [11]. The inspiratory effort, gravity and gender differences may alter the area of the low attenuation area (LAA%) as well as the high attenuation area (HAA%). Therefore, these factors should be considered during the interpretation in normal patients as well as patients with lung diseases.

THE ASEAN JOURNAL OF RADIOLOGY
ISSN 2672-9393

Materials and methods

This was a retrospective cross-sectional study conducted in the Radiology Department of Universiti Kebangsaan Malaysia Medical Center (UKMMC), analysing CT images and plain chest radiographs done for patients in the age group of 13 – 85 years old from 1st January 2015 to 20th June 2015. The universal sampling method was used and there were a total of 462 CT Thorax imaging cases performed in this period. Among the 462 sets of CT images, 184 CT were reported as lung fibrosis and infections, 86 CT were reported as lung malignancy or lung metastasis, 69 CT were associated with granuloma or atelectatic changes and 58 CT were associated with breathing artefacts. It was found that 65 sets of CT images were reported to be normal while 3 sets of images were performed on non-Malaysian citizens and therefore were excluded. In conclusion, a total of 62 sets of CT images (n=62) were included in this study.

Imaging techniques of CT scans and chest radiographs

CT Thorax was conducted using a CT scanner, Siemens CT Somatom Sensation 64 (64 slices) of the helical mode in the craniocaudal direction. The patient was in a supine position during the scanning and a standard instruction in respective dialects was given to the patient: taking a deep breath and holding the breath. Images were acquired during inspiration. An approximately 1.0 - 1.5 ml/kg contrast material was injected via an intravenous assess at the upper limb with the flow rate of 2.5 - 5 mls/s. An image was acquired with 120 kVp, 200 mAs, one millimeter reconstruction (1 mm slice thickness), B30 and B70 reconstruction kernel using software Syngo CT 2006A.

A chest radiograph was carried out using Xray machine computed radiography unit, Digital Diagnost Philips Medical Systems with 100 - 110 kVp, 4 – 8 mAs exposure with the presence of grid and filter. The patient was in a standing position with his chest facing the detector. An AP view of the radiograph was acquired given the patient was unable to stand erect during the examination.

All CT and Plain radiograph images were interpreted using DICOM viewer OsiriX Lite.

Lung attenuation measurement from CT scans

Mean lung parenchymal attenuation (MLA) of these 62 sets of images was analysed to measure lung attenuation at the lung apex (Figure 2a), the main carinal level (MCL) at anterior, middle and posterior regions bilaterally (Figure 2b) and the lung base level (BL) at anterior, middle and posterior regions (Figure 2c and 2d) bilaterally. The sampling location for MLA at MCL (middle) and BL (middle) was at the mid clavicular line, with additional imaginary lines to divide the lungs into anterior 1/3, middle 1/3 and posterior 1/3. The region of interest (ROI) for the measurement is round in shape and is fixed constant with an area of 1.0 cm^2 ± 0.2 cm^2. The ROI was placed at the lung parenchymal by avoiding large vessels.

Lung volume estimation calculation

There were a total of 26 patients from the 62 study subjects who had a chest radiograph within six months from the date of CT acquisition. These was a quantitative measurement of the total lung volume methods used in the calculations:

i. Predictive equation published by Konheim:
Predicted TLV (pTLV) = [-630.819 + (967.100*Gender) + (25.197*Height) - (713.838*Race) + (15.103*Age)]/1000; Gender: Male (1), Female (0); Race: African American (1), others (0); Height in cm, Age in years.

ii. Estimation from frontal radiograph, as published by Canals M (Figure 1).

iii. Ellipsoid formula (a summation of right and left lung volumes of 0.52xAPxWxCC) based on the measurement from CT images. The AP and width diameter of both lungs was measured at lung bases, whereas for the craniocaudal measurement, it was measured by drawing a line from the apex to the posterior medial most of the costophrenic angles shown in (Figure 3a, 3b, 3c & 3d). This is a modified method after considering previous publications suggested by other authors. Some authors use the ellipsoid formula in their complex calculations. According to Canals M's formula: $V^*_L = 0.496 \cdot V_{RX}$, shows a possible similarity or a correlation to the previously published calculations, where it could be correlated with ellipsoid formula: Volume, $V = 0.523 \cdot a \cdot b \cdot c$; whereby a, b and c are the diameters of the ellipsoid.

THE ASEAN JOURNAL OF RADIOLOGY
ISSN 2672-9393

iv. Semi auto-segmentation and volumetric calculation using DICOM compatible program, OsiriX Lite. The lungs were differentiated into right and left lungs with the dead space (air in the trachea and bronchus) and major blood vessels excluded in the calculation (Figure 4a, 4b, 4c, 4d, 4e & 4f). Correlations between these four methods were made.

Statistical analysis

T test was used to determine a statistical difference of MLA of both lungs. Subsequently, the independent T test was used to determine the statistical significance of MLA among female and male data. Pearson-correlation was used to analyse the correlation of the four methods of the total lung volume estimations i.e. based on predicted calculations (method i), the frontal chest radiograph (method ii), the ellipsoid formula with measurement from CT images (method iii) and volumetry calculation using DICOM compatible program, OsiriX (method iv). A statistical analysis was done using IBM SPSS Statistics 20.

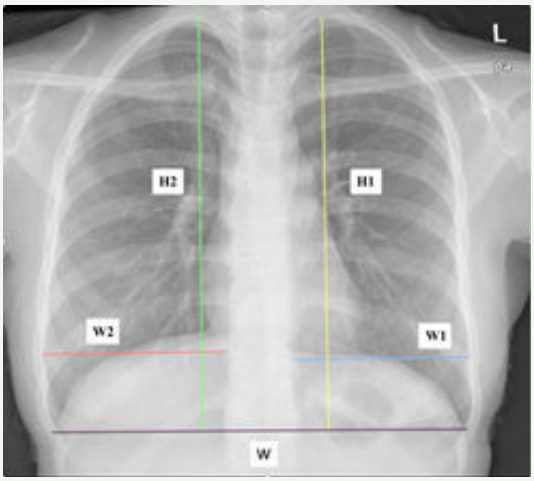

Figure 1. *Frontal radiograph displays the reference line for calculation of V_{RX}. (reproduced referring to Canal et. al [9]).*
W: straight line width between two costophrenic recesses
H1: height from W to the top of left lung
H2: height from W to the top of right lung
W1: left lung width at the midpoint of the diaphragm dome
W2: right lung width at the midpoint of the diaphragm dome

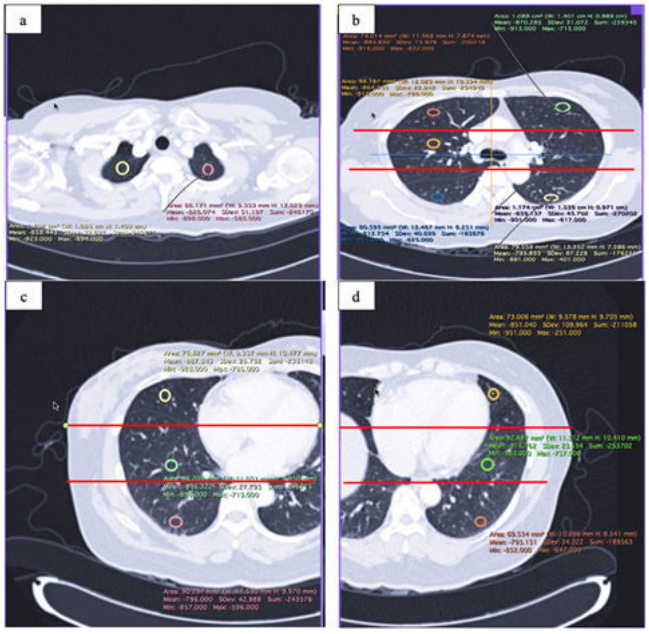

Figure 2. *Multiplanar reformat shows lung attenuation of apical regions (a), main carinal level (anterior, mid and posterior) (b) and at base level (anterior, mid and posterior) of right (c) and left lungs (d).*

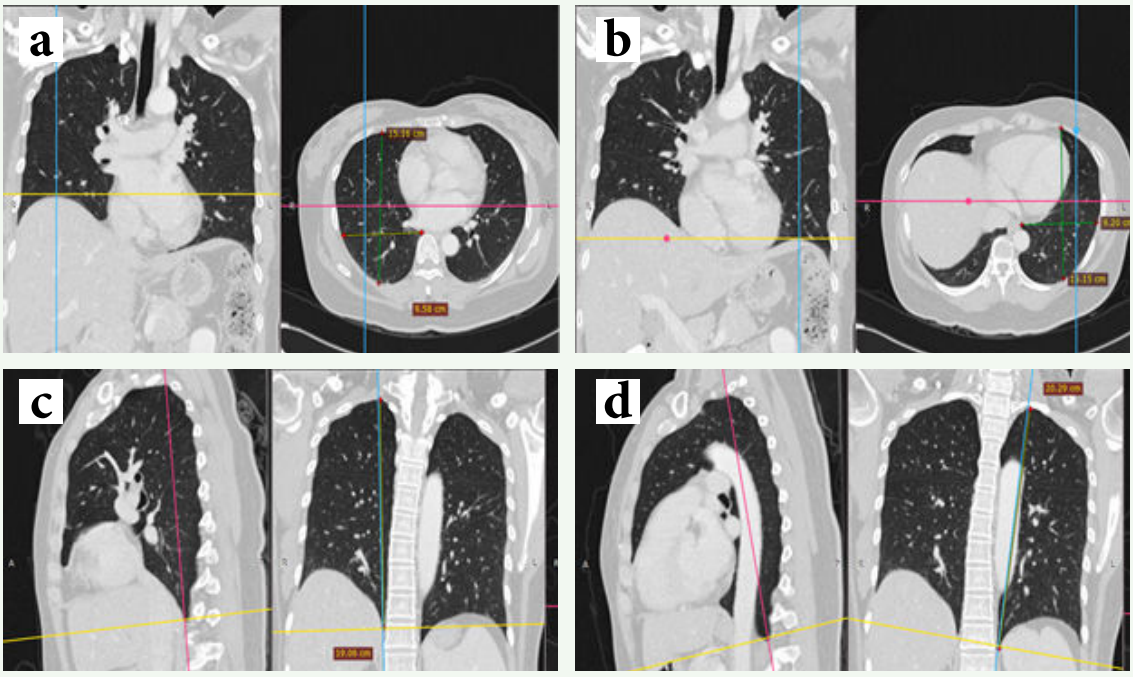

Figure 3. *Multiplanar reformat shows measurement of AP diameter and width of right (a) and left (b) lungs and craniocaudal measurement of right (c) and left (d) lungs.*

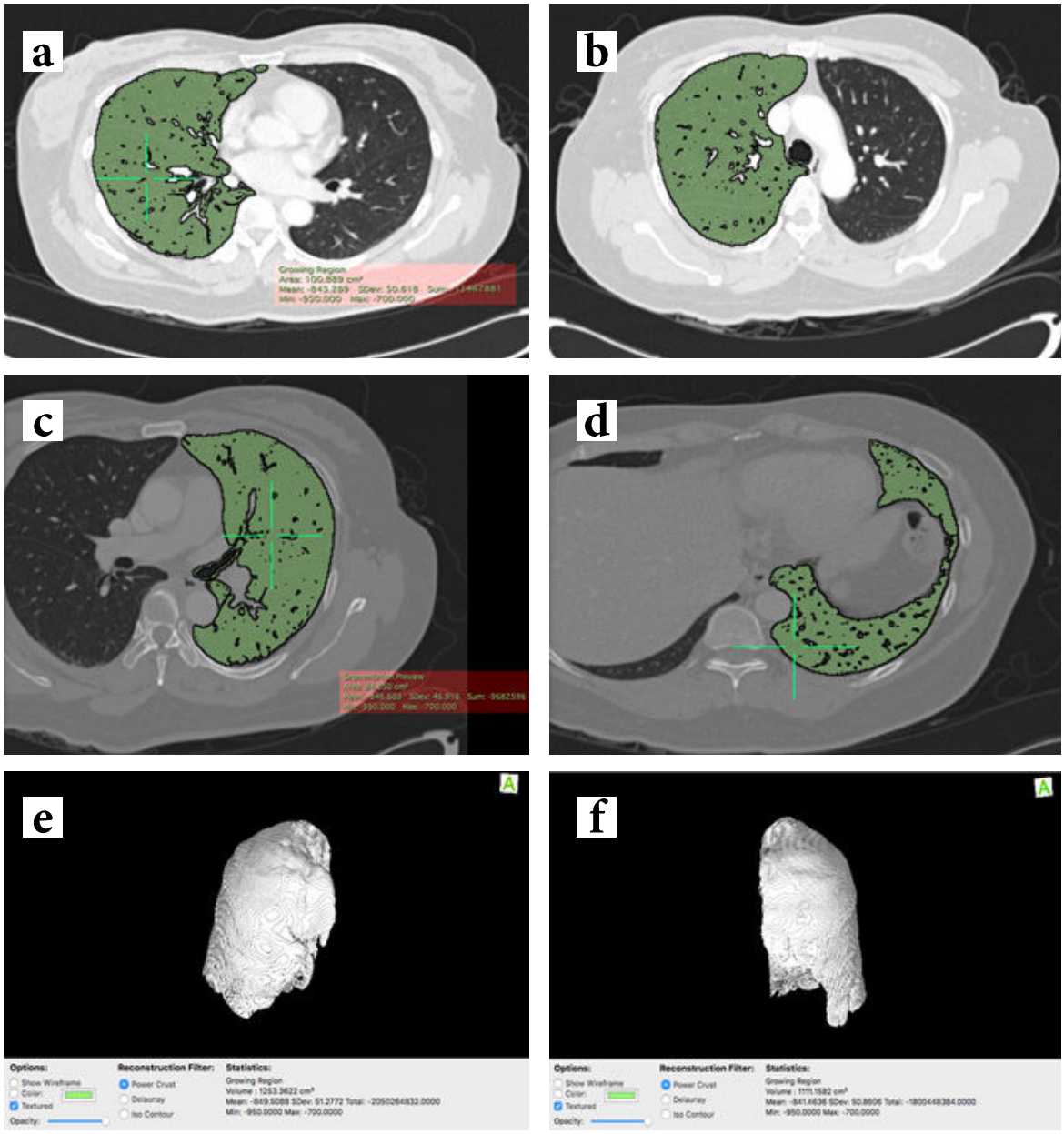

Figure 4. *Images show semi auto-segmentation of right (a, b) and left (c, d) lungs with the right (e) and left (f) lung volume calculations using DICOM compatible program, OsiriX Lite.*

Results

There are 62 sets of CT images included in this study. Majority of the CT images were done for Malay patients (n = 38, 61%), followed by Chinese (n = 18, 29%), Indian (n = 4, 6%), Orang Asli and Kadazan (n = 1, 2%) respectively, as shown in Figure 5.

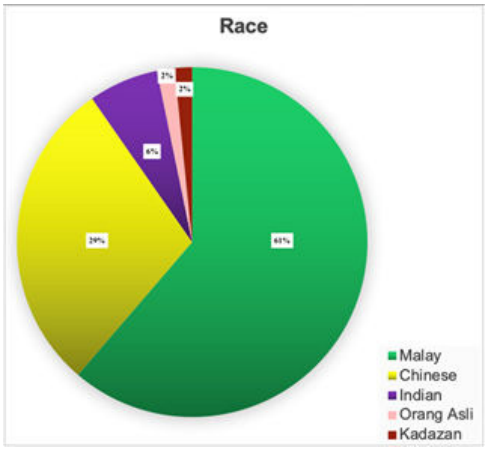

Figure 5. *Demographic data based on different race.*

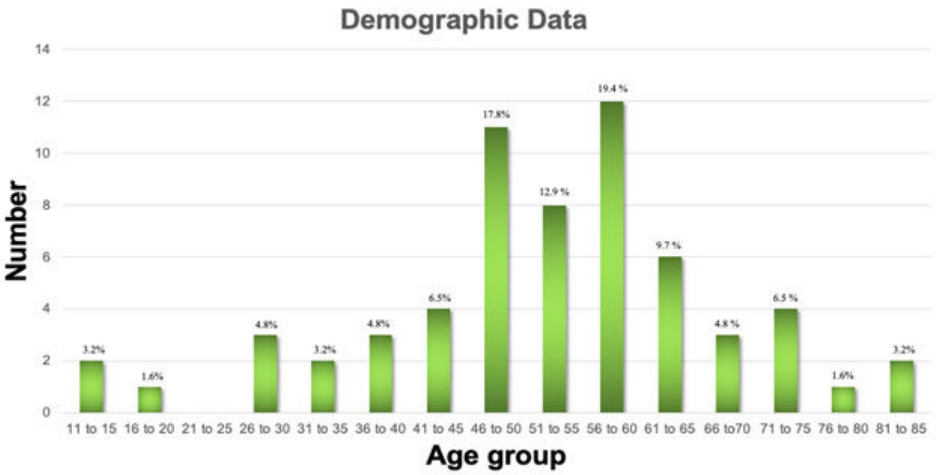

Figure 6. *Demographic data based on age groups.*

THE ASEAN JOURNAL OF RADIOLOGY
ISSN 2672-9393

Lung parenchymal attenuation

There were a total of 62 sets of CT images (n = 62) analysed for lung attenuation, with 34 female patients and 28 male patients. Demographic data was classified based on race and age group of the study subjects (Figure 5 and 6).

The mean of lung parenchymal attenuation (MLA) of both lungs at apical, main carinal levels (anterior, middle and posterior) and at a base level (anterior, middle and posterior) is shown in Table 1.

Table 1. *Mean lung attenuation of 62 subjects with T test result.*

Lung locations	Lung attenuation (HU), mean ± SD	Comparing with	P
R Apex (-HU)	821.77 ± 8.67	R Middle MCL (-HU)	< 0.05
R Anterior MCL (-HU)	849.23 ± 9.41	R Middle MCL (-HU)	< 0.05
R Middle MCL (-HU)	838.85 ± 9.67	R Middle BL (-HU)	< 0.05
R Posterior MCL (-HU)	802.39 ± 12.9	R Middle MCL (-HU)	< 0.05
R Anterior BL (-HU)	860.26 ± 9.52	R Middle BL (-HU)	< 0.05
R Middle BL (-HU)	823.53 ± 11.4	R Middle MCL (-HU)	< 0.05
R Posterior BL (-HU)	787.66 ± 14.8	R Middle BL (-HU)	< 0.05
L Apex (-HU)	819.76 ± 8.62	L Middle MCL (-HU)	< 0.05
L Anterior MCL (-HU)	845.6 ± 10	L Middle MCL (-HU)	< 0.05
L Middle MCL (-HU)	834.16 ± 10.6	L Middle BL (-HU)	< 0.05
L Posterior MCL (-HU)	806.42 ± 11.2	L Middle MCL (-HU)	< 0.05
L Anterior BL (-HU)	842.65 ± 11.2	L Middle BL (-HU)	< 0.05
L Middle BL (-HU)	816.44 ± 11.8	L Middle MCL (-HU)	< 0.05
L Posterior BL (-HU)	789.66 ± 14	L Middle BL (-HU)	< 0.05

**R = right, L = left, MCL = main carina level, BL = base level*

For the right and the left lungs, the differences in MLA at the middle MCL vs the apex and the middle MCL vs middle BL were statistically significant ($p<0.05$). At the main carina level, the MLA values at the anterior vs the middle and the posterior vs the middle parts revealed a statistically significant difference ($p<0.05$). At the base level, the differences in the MLA value at the anterior vs the middle and the posterior vs the middle parts also showed statistical significance ($p<0.05$). Additionally, MLA of both lungs for male and female at the apical, main carinal level (anterior, middle and posterior) and at the base level (anterior, middle and posterior) was tabulated in Table 2.

Table 2. *Mean lung attenuation of male and female with independent T test result.*

Lung locations	Lung attenuation (HU), mean ± SD		P
	Male (n = 28)	Female (n = 34)	
R Apex (-HU)	828.68 ± 12.7	816.09 ± 11.7	0.158
R Anterior MCL (-HU)	862.54 ± 11.1	838.26 ± 13.6	< 0.05
R Middle MCL (-HU)	854.14 ± 11.5	826.26 ± 13.6	< 0.05
R Posterior MCL (-HU)	819.43 ± 15	788.35 ± 19	< 0.05
R Anterior BL (-HU)	873.89 ± 13.1	849.03 ± 12.5	< 0.05
R Middle BL (-HU)	835.39 ± 16	813.76 ± 15.6	0.065
R Posterior BL (-HU)	799.07 ± 17.2	778.26 ± 22.7	0.172
L Apex (-HU)	826.32 ± 13.9	814.35 ± 10.6	0.178
L Anterior MCL (-HU)	864.36 ± 11.1	830.15 ± 13.9	< 0.05
L Middle MCL (-HU)	851.25 ± 14	820.09 ± 14	< 0.05
L Posterior MCL (-HU)	818.89 ± 15.6	796.15 ± 15.3	< 0.05
L Anterior BL (-HU)	854.71 ± 14.2	832.71 ± 16.1	0.054
L Middle BL (-HU)	833.5 ± 16	802.38 ± 15.7	< 0.05
L Posterior BL (-HU)	803.21 ± 15.4	778.5 ± 21.7	0.086

**R = right, L = left, MCL = main carina level, BL = base level*

THE ASEAN JOURNAL OF RADIOLOGY
ISSN 2672-9393

Lung Volume Estimation

The mean of the estimated total lung volume using method i was 4717.58 ± 276 ml (95% CI 4440 – 4990), method ii was 4086.96 ± 446 ml (95% CI 3640 – 4530), method iii was 3903.27 ± 448 ml (95% CI 3460 – 4350), whereas method iv was 2864.54 ± 345 ml (95% CI 2520 – 3210). Based on method i, the range of the lung volume for the study population ranged between 3476 until 5884 ml. (Table 3)

Quantitative estimations of the total lung volume using four methods are summarized in a scatter plot and it showed positive linear relations (Figure 7a - f).

A moderate to strong correlation was observed between the estimation of the total lung volume using these 4 methods: method i versus ii ($r = 0.679$; $p < 0.005$, 95% CI, 0.396 - 0.844), method i versus iii ($r = 0.655$; $p < 0.005$, 95 % CI, 0.359 - 0.831), method i versus iv ($r = 0.565$; $p < 0.005$, 95% CI, 0.228 – 0.781), method ii versus iii ($r = 0.782$, $p < 0.005$, 95% CI, 0.567 - 0.897), method ii versus iv ($r = 0.745$; $p < 0.005$, 95% CI, 0.503 - 0.878) and method iii versus iv ($r = 0.899$ $p < 0.005$, 95% CI, 0.786 – 0.954) (Table 4).

Table 3. *Estimations of total lung volume (in unit mls) with 4 different methods.*

Estimation methods	Total lung volume (ml)			
	Min	Max	Mean	95 % CI
Calculating total volume using formula by Konheim et al.	3476	5884	4717.58 ± 276	4440 – 4990
Estimating lung volume using formula by Canals et al. (Chest X-Ray)	2076	7669	4086.96 ± 446	3640 – 4530
Estimating total lung volume using Ellipsoid formula (0.52xAPxWxCC)	1938	6222	3903.27 ±448	3460 – 4350
Calculating lung volume using semi automatic segmentation with CT images	1187	4267	2864.54 ± 345	2520 – 3210

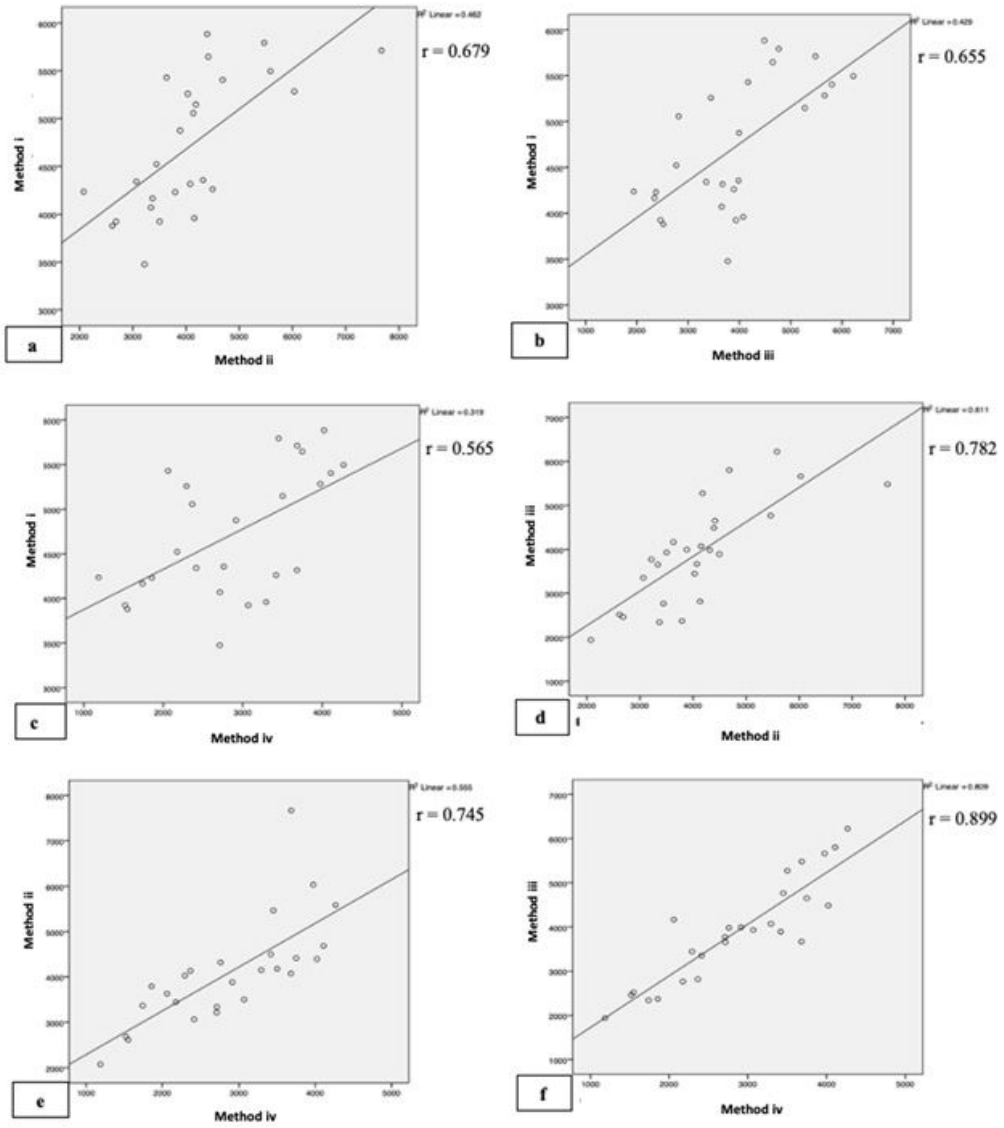

Figure 7. *(a) Positive correlation between calculated total lung volume using method i and ii, (b) using method i and iii, (c) using method i and iv, (d) using method ii and iii, (e) using method ii and iv, and (f) using method iii and iv.*
**Method i: Calculated total volume using formula by Konheim et al, Method ii: Estimated lung volume using formula by Canals et al (Chest X-Ray), Method iii: Estimated total lung volume using Ellipsoid formula (0.52xAPxWxCC), Method iv: Calculated lung volume using semi auto segmentation with CT images.*

Table 4. *Pearson Correlations between estimations of total lung volume with 4 different methods.*

Estimation methods*	Pearson correlation**				p-value***			
	Method i	Method ii	Method iii	Method iv	Method i	Method ii	Method iii	Method iv
Method i	1	.679	.655	.565		.000	.000	.003
Method ii	.679**	1	.782**	.745**	.000		.000	.000
Method iii	.655	.782	1	.899	.000	.000		.000
Method iv	.565	.745	.899	1	.003	.000	.000	

**Method i: Calculating total volume using formula by Konheim et al., Method ii: Estimating lung volume using formula by Canals et al. (chest X-ray), Method iii: Estimating total lung volume using Ellipsoid formula, Method iv: Calculating lung volume using semi automatic segmentation with CT images.*
***Correlation is significant at the 0.01 level (2-tailed).*
****Sig. (2-tailed)*

Discussion

The quantitative measurement of mean lung parenchymal attenuation (MLA) among Malaysian citizens with normal chest CT and methods of total lung volume estimations are described in this study.

Lung attenuation

Differences in MLA during inspiration in relation to the location of the lung, were described in previous studies [5,11]. In this study, MLA at the middle main carinal level (MCL-M) was lower than the value at the apex and the middle base level (BL-M). At MCL, MLA at anterior MCL (MCL-A) was the lowest followed by MCL-M and posterior MCL (MCL-P); whereas at the base level, MLA at the anterior base level (BL-A) was also the lowest followed by BL-M and the posterior base level (BL-P).

MLA at MCL was lower compared to the apex and could be related to more chest expansion at the carinal level compared to a relatively fixed apex [5]. MLA was higher in BL compared to MCL probably also related to better chest expansion at MCL. The variation seen across MCL and BL (anterior, middle and posterior) could be related to the supine position during image acquisition as the chest expansion at the posterior part of the chest is reduced compared to the anterior part of the chest. Chest expansion or lung volume measurement in the sitting position (using the single breath gas dilution method) was found greater than in the supine position, as in during the CT scan [11]. Therefore, in the supine position, lung expansion is reduced with the most affected part located posteriorly, as seen in this study, whereby, MLA of the posterior part of the lung (MCL-P and BL-P) was higher than the middle (MCL-M and BL-M) and the anterior part (MCL-A and BL-A) at the same corresponding levels. This finding was also observed in the previous study and the MLA regional differences could be related to the lung volume, chest expansion or inflation and gravity influence on the blood flow [3, 12].

According to a study conducted by Smit et al., there was no statistical difference in MLA due to gender differences [5]. However, the low attenuation area in male was found larger compared to females in a study conducted among Chinese population [11]. According to Kim et al., quantitative variation due to gender differences was significant in his study [13]. In this study, it was observed that the MLA of males was lower than females' in both lungs, at the apex, MCL and BL bilaterally. It was a statistically significant variation of MLA due to gender differences ($p<0.05$) at MCL (anterior, middle and posterior) bilaterally, right BL-A and left BL-M. The possible explanation for lower MLA in males could be related to a larger lung volume [11] and more chest expansion compared to females [14] as males were found to have a larger thoracic rib cage [15]. Even though the ratio of the alveoli amount over a standard unit area or volume was similar in both sexes, males were found to have a higher amount of alveoli than females in general [15]. This is however, the variation due to gender differences at both apical regions and BL-P showed no statistical significance ($p>0.05$), which could be related to a poor degree of expansion at these regions in both females and males.

THE ASEAN JOURNAL OF RADIOLOGY
ISSN 2672-9393

Lung Volume Estimation

Lung volume was generally higher among males, taller and thinner individuals [11]. There are prediction formulas for the total lung volume estimations published and some of these equations take into consideration of an individual's height [10 & 11], gender [10 & 11], age [10], race [10] and weight [11].

The lung volume for the study population ranged from 3476 to 5884 mls with the mean of 4717.58 mls (95% CI 4440 – 4990) using method i; Predicted TLV (pTLV) = [-630.819 + (967.100*Gender) + (25.197*Height) - (713.838*Race) + (15.103*Age)]/1000; Gender: Male (1), Female (0); Race: African American (1), others (0); Height in cm, Age in years. The mean of the 2nd, 3rd and 4th methods was lower compared to the 1st method, but the 2nd and 3rd methods showed a 95% confidence interval of 3640 – 4530 mls and 3460 – 4350 mls, respectively, whereby the upper limit values were relatively closer to the lower limit value of the 1st method. The mean of the estimated lung volume using method ii, iii and iv was found to be lower and this could be attributable to positioning and inspiratory effort during image acquisition. For method iv, the airway and blood vessels' volume were not included and this is another additional explanation leading to a lower estimated lung volume mean.

A moderate to strong correlation (r value range from 0.565 until 0.899) was seen between all the four different estimation methods described [16]. Method i has a simple method to estimate the lung volume by filling in demographic data of the patient such as gender, height, race and age, without the need of any invasive intervention.

Method ii required information from a frontal chest radiograph. A plain chest radiograph was a routine pre-operative workout prior to anaesthesia administration in some centres [16,17]. The total lung volume could be estimated without any additional unnecessary radiation to the patients, as all patients will have a baseline chest radiograph done prior to their operation. However, some authors do not recommend a chest radiograph as a routine preoperative workout without a clear clinical indication [17 & 18].

Ellipsoid formula and measurement from CT images (Anterior-posterior distance, width and cranio-caudal length) were used in method iii. This method yielded a positive linear correlation with other methods of total lung estimations (with method i, ii and iv). Even without a sophisticated software for auto-segmentation and calculation of the lung volume, estimation of the total lung volume from CT images was possible by using ellipsoid formula.

Comparing all the 4 methods for lung volume estimation, method iv showed the lowest mean value, as the chest expansion of an individual was reduced on the supine position, during CT scan examination. This may not be as accurate compared to method i and ii. Method i only required demographic data from the patient, whereas method ii needed data from a frontal chest radiograph, which was a routine pre-operative examination done in most centres. By considering the risk from radiation exposure, method ii was as good as method i due to no additional radiation given to the patient.

In the occasion when a CT scan examination was already done for the patient with the absence of a sophisticated software to do auto-segmentation and lung volume auto-calculation, method iii (ellipsoid formula) could be used to estimate the lung volume easily.

Several limitations were encountered in this study. Smoking history was not considered during data collection and this could also be one of the factors in causing variation in mean lung attenuation [11] although a study by Smit et al., showed no correlation of smoking or number of pack years with lung attenuation [5].

In this study, four different methods of total lung volume estimation were derived and the correlations between these four methods were demonstrated. The estimations of the lung volume using calculation for the chest radiograph and CT images could be lower compared to the spirometry or body plethysmography due to variation in chest expansion in sitting versus the supine position [11]. During CT image acquisition, there were challenges to ensure all patients were in their maximum effort of full inspiration [10].

THE ASEAN JOURNAL OF RADIOLOGY
ISSN 2672-9393

To further strengthen the next related projects, it is suggested to correlate the study of mean lung parenchymal attenuation (MLA) with smoking history and differences in lung attenuation changes during respiration such as during full inspiration and forceful expiration. The correlation of lung volume estimation methods can be made with findings in spirometry, body plethysmography or gas dilution technique, in a prospective trial in the future.

Conclusion

MLA at MCL was lower than the apex and the base level bilaterally. It was also lower at the anterior part compared to the middle and the posterior part at MCL and BL. This could be related to better chest expansion and inspired air distribution at the MCL. The posterior part of the lungs showed higher lung attenuation which was likely related to the position during scanning, a lesser degree of chest expansion at the posterior part of the lung and gravity influences. Generally, MLA of the male subjects was lower than females, except at both apices and part of the lung bases. Lung volume estimations using methods i, ii, iii and iv showed a linear positive moderate to strong correlation among all the four methods. Therefore, it was possible to estimate the total lung volume using demographic data, a plain chest radiograph or ellipsoid formula.

The area of low attenuation (LAA%) and high attenuation area (HAA%) could be affected by inspiratory effort, gravity and gender differences. Therefore, these factors should be considered during the interpretation of LAA% and HAA% in normal patients as well as patients with lung diseases.

This study could help to generate data for future references for lung parenchymal attenuation and the lung volume particularly for Malaysia or Southeast Asia.

Ethics

This study was approved by the Universiti Kebangsaan Malaysia Research and Ethics Committee, numbered FF-2018-327.

Acknowledgement

The authors would like to express their greatest gratitude to Dr. Norzailin Abu Bakar, Dr. Dyah Ekashanti, Dr. Sarawana and all the staff in the UKMMC Radiology Department, particularly to radiologists, radiographers and colleagues who contributed their valuable opinions and continuous support towards the completion of this study.

THE ASEAN JOURNAL OF RADIOLOGY
ISSN 2672-9393

References

1. Whiting P, Singatullina N, Rosser JH. Computed tomography of the chest: I. Basic principles. BJA Educ 2015;15:299-304. doi:10.1093/bjaceaccp/mku063.

2. Haas M, Hamm B, Niehues SM. Automated lung volumetry from routine thoracic CT scans: how reliable is the result? Acad Radiol 2014;21:633-8. doi: 10.1016/j.acra.2014.01.002.

3. Stein JM, Walkup LL, Brody AS, Fleck RJ, Woods JC. Quantitative CT characterization of pediatric lung development using routine clinical imaging. Pediatr Radiol 2016;46:1804-12. doi: 10.1007/s00247-016-3686-8.

4. Zach JA, Newell JD Jr, Schroeder J, Murphy JR, Curran-Everett D, Hoffman EA, et al. Quantitative computed tomography of the lungs and airways in healthy nonsmoking adults. Invest Radiol 2012;47:596-602. doi: 10.1097/RLI.0b013e318262292e.

5. Smit HJ, Golding RP, Schramel FM, Devillé WL, Manoliu RA, Postmus PE. Lung attenuation measurements in healthy young adults. Respiration 2003;70:143-8. doi: 10.1159/000070060.

6. Kauczor HU, Hast J, Heussel CP, Schlegel J, Mildenberger P, Thelen M. CT attenuation of paired HRCT scans obtained at full inspiratory/expiratory position: comparison with pulmonary function tests. Eur Radiol 2002;12:2757-63. doi: 10.1007/s00330-002-1514-z.

7. Schlesinger AE, White DK, Mallory GB, Hildeboldt CF, Huddleston CB. Estimation of total lung capacity from chest radiography and chest CT in children: comparison with body plethysmography. AJR Am J Roentgenol 1995;165:151-4. doi: 10.2214/ajr.165.1.7785574.

8. Reger RB, Young A, Morgan WK. An accurate and rapid radiographic method of determining total lung capacity. Thorax 1972;27:163-8. doi: 10.1136/thx.27.2.163.

9. Canals M, Olivares R, Rosenmann M. A radiographic method to estimate lung volume and its use in small mammals. Biol Res 2005;38:41-7. doi: 10.4067/s0716-97602005000100006.

10. Konheim JA, Kon ZN, Pasrija C, Luo Q, Sanchez PG, Garcia JP, et al. Predictive equations for lung volumes from computed tomography for size matching in pulmonary transplantation. J Thorac Cardiovasc Surg 2016;151:1163-9. doi: 10.1016/j.jtcvs.2015.10.051.

11. Cheng T, Li Y, Pang S, Wan H, Shi G, Cheng Q, et al. Normal lung attenuation distribution and lung volume on computed tomography in a Chinese population. Int J Chron Obstruct Pulmon Dis 2019;14:1657-68. doi: 10.2147/COPD.S187596.

12. Lee KN, Yoon SK, Sohn CH, Choi PJ, Webb WR. Dependent lung opacity at thin-section CT: evaluation by spirometrically-gated CT of the influence of lung volume. Korean J Radiol 2002;3:24-9. doi: 10.3348/kjr.2002.3.1.24.

13. Kim SS, Jin GY, Li YZ, Lee JE, Shin HS. CT quantification of lungs and airways in normal Korean subjects. Korean J Radiol 2017;18:739-48. doi:10.3348/kjr.2017.18.4.739.

14. Adedoyin R, Adeleke OE, Fehintola AO, Erhabor G, Bisiriyu L. Reference values for chest expansion among adult residents in Ile-Ife, Nigeria- a cross-sectional study. J Phys Ther 2013;6:54-8. doi:10.4172/2157-7595.1000113.

15. LoMauro A, Aliverti A. Sex differences in respiratory function. Breathe (Sheff) 2018;14:131-40. doi:10.1183/20734735.000318.

THE ASEAN JOURNAL OF RADIOLOGY
ISSN 2672-9393

16. Akoglu H. User's guide to correlation coefficients. Turk J Emerg Med 2018;18:91-3. doi: 10.1016/j.tjem.2018.08.001.

17. Kovacevic M, Goranovic T, Markic A, Jelisavac M, Zuric I, Tonkovic D. Usefulness of routine chest X-ray in preoperative evaluation of patients undergoing non-cardiopulmonary surgery: a prospective observational study:1AP5-5 [abstract]. Eur J Anaesthesiol 2012;29 Suppl 50:16.

18. Young EM, Farmer JD. Preoperative chest radiography in elective surgery: review and update. S D Med 2017;70:81-7.

Case Report

Delayed pneumomediastinum: A rare subacute complication of paraquat poisoning

Tashi Gyeltshen, M.D.[(1)]
Kinley Sangay Dorji, M.D.[(2)]
Nidup, M.D.[(1)]
From [(1)] Department of Imaging and Radio-diagnosis,
Jigme Dorji Wangchuck National Referral Hospital (JDWNRH),
Thimphu, Bhutan.
[(2)] Eastern Regional Referral Hospital, Mongar, Bhutan.
Address correspondence to K.S.D. (e-mail: kinleysangay1323@gmail.com)

Received 14 June 2021 ; revised 31 July 2021 ; accepted 5 September 2021
doi:10.46475/aseanjr.v22i3.134

Abstract

Paraquat (PQ) is a non-selective widely used weedicide. Paraquat poisoning has a high mortality rate with no available antidote as of now. It is rare in Bhutan, but mostly discovered in the southern part of the country. Patients usually present with multi-organ failures such as respiratory, liver, and renal failures. This is a case report of a 24-year-old female referred with a history of paraquat ingestion. Initially, she complained of epigastric and retrosternal chestpain with excoriation of the oral mucosa. She later developed acute kidney injury and respiratory distress. Chest CT revealed pneumomediastinum, massive bilateral pneumothoraces, and subcutaneous emphysema. Although there have been few reported cases of pneumomediastinum with or without pneumothorax and subcutaneous emphysema, most of them have an acute presentation (less than 1 week).

Keywords: Paraquat, Poisoning, Complication, Pneumomediastinum, Pneumothorax.

THE ASEAN JOURNAL OF RADIOLOGY
ISSN 2672-9393

Case summary

A 24-year-old female was admitted to the emergency department (ED) with an alleged history of deliberate self-harm in which she consumed around 15-20 ml of PQ at her home. She was initially seen at her local hospital and was referred to the district hospital on the same night. In the district hospital, the patient was given intravenous (IV) fluids, H2 blocker, antiemetic, steroids, and IV antibiotics (ceftriaxone and metronidazole). On admission at ED, she complained of retrosternal and epigastric pain (burning type) and shortness of breath on exertion. She had a history of migraines and no past psychiatric history. There was no fever, nausea, vomiting, diarrhea, or cough. Urine output was adequate at the time of admission. On examination, she was afebrile and anicteric with mild facial swelling. There was excoriation of oral mucosa and around the lower lip. Her GCS was 15/15 and all her vital signs were stable. The auscultation of the lung revealed few bilateral basal crepitations. The neurological, cardiovascular, and abdominal systems were unremarkable. Her blood report at the time of the admission showed neutrophil leukocytosis (WBC-21930 μ/mL, neutrophil-89.2%). Her renal function test showed raised urea and creatinine level, about 165 mg/dL and 4.7 mg/dL, respectively, and low potassium (3.3 mEq/L) suggestive of acute kidney injury (AKI). The rest of her investigation was unremarkable.

Initial standard CXR anteroposterior (AP) view revealed patchy infiltration involving bilateral lower lobes with pleural effusion. No evidence of pneumothorax, pneumomediastinum, or subcutaneous emphysema (Figure 1).

Figure 1. *Chest X ray anteroposterior(AP) view showing patchy infiltration involving bilateral lower lobes with pleural effusion.*

She was admitted to the medical ward where they established a central line and urgent hemodialysis was performed. IV steroids and ceftriaxone were continued. With regular hemodialysis and potassium chloride (KCl) solution, her AKI and hypokalemia improved. The subsequent abdomen ultrasound showed bilateral increased renal cortical echoes, in line with kidney insult, and bilateral pleural effusion. Echocardiography showed mild left ventricular hypertrophy (LVH) and tricuspid regurgitation (TR) with small pericardial effusion. The systolic function was normal.

Then on the 20th day of the admission, she developed respiratory distress and was given high flow oxygen. The urgent computed tomography of the chest was performed which revealed massive subcutaneous emphysema, bilateral pneumothoraces, and pneumomediastinum with collapse-consolidation of both lungs (Figure 2).

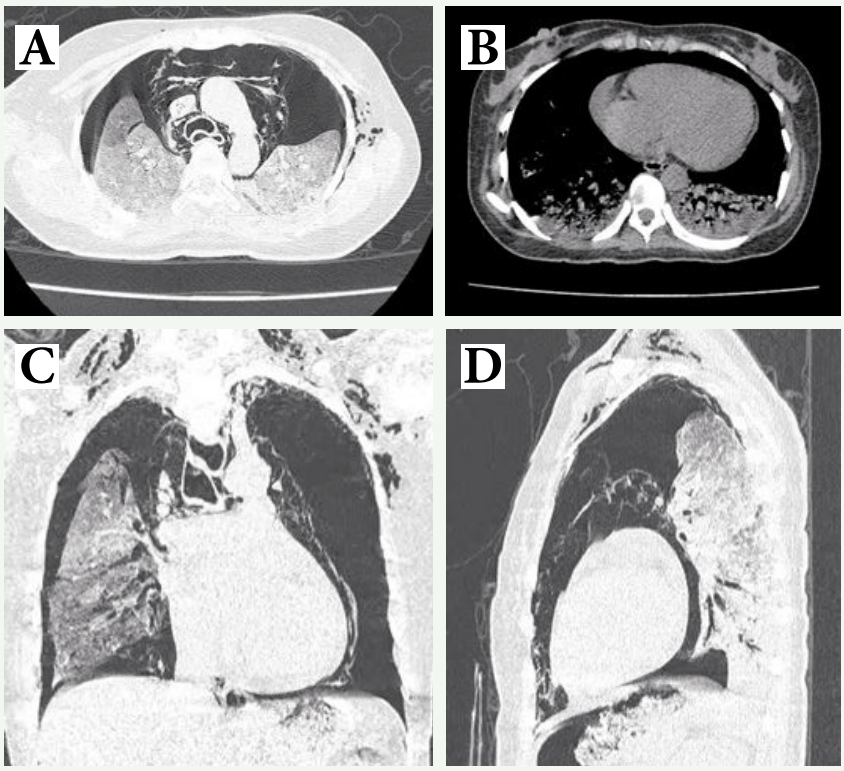

Figure 2. *Plain CT Chest A) axial (lung window), B) axial (mediastinal window), C) coronal (lung window) and D) sagittal (lung window) showing pneumo-mediastinum subcutaneous emphysema, bilateral pneumothoraces and with collapse-consolidation of both lungs.*

THE ASEAN JOURNAL OF RADIOLOGY
ISSN 2672-9393

The patient was immediately transferred to the adult intensive care unit (AICU) in view of impending type 2 respiratory failure. She was intubated and bilateral intercostal drainage (ICD) was inserted (Figure 3). However, the patient expired on the same day in the evening.

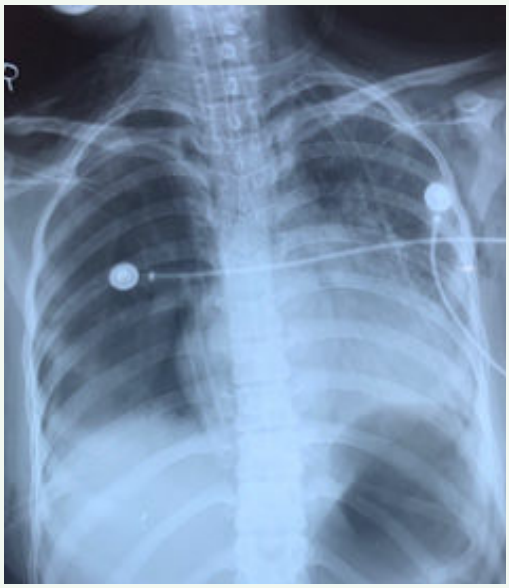

Figure 2. *Chest X-ray anteroposterior (AP view) showing bilateral pneumothoraces, pneumomediastinum, subcutaneous emphysema and consolidation in both lungs with endotracheal tube and bilateral intercostal drainage tubes.*

Discussion

Paraquat (N, N'-dimethyl-4, 4'-bipyridinium dichloride) is a non-specific weedicide that has broad-spectrum effects, rapid deactivation on contact with soil, and is relatively inexpensive. Due to these favorable characteristics, it is a widely used weedicide which is frequently abused with lethal consequences. It is a leading cause of fatal poisoning in many parts of Asia, Pacific nations, and the Americas [1]. Paraquat poisoning is rare in Bhutan but is mostly discovered in the southern part of the country. In Bhutan, PQ is not an approved weedicide according to National Plant Protection Centre (NPPC) [2].

PQ intoxication results in multi-systemic toxicity with early manifestation seen in the gastrointestinal tract, kidney, liver, and lungs [3]. The toxic effect of PQ is thought to be caused by the production of free radicals which damage cell membrane resulting in a wide spectrum of cellular, structural and functional abnormalities [4].

PQ poisoning can either be accidental and deliberate, although in most cases it is deliberate [5]. Following ingestion, early symptoms of PQ poisoning include burning sensation in the throat, abdominal pain, nausea, vomiting, and diarrhea. There can be excoriation and ulcerations of the tongue, oral mucosa, and esophagus due to its caustic effect [6]. If the patient has ingested 4mg/kg or more, it can lead to multi-organ failures such as renal, liver, and respiratory failures. Likewise, in our case, the patient complained of retrosternal and epigastric pain (burning type), shortness of breath on exertion with excoriation of oral mucosa and around the lower lip. Later on, she developed oliguria with a deranged renal function test suggestive of acute kidney injury.

The most common affected system in PQ ingestion is the respiratory system. This could be due to the increased concentration of PQ and low concentration of antioxidant levels in the lungs [4,7]. Following ingestion of PQ, initially, there is a destructive phase characterized by damage of alveolar epithelium, hemorrhage, and congestion which will manifest as diffuse ground-glass opacities and consolidation on imaging. In some rare cases, a patient can have an acute presentation of pneumomediastinum with or without pneumothorax and subcutaneous emphysema as demonstrated Daisley et al [4], Im et al[6] and Chen et al [8]. Our patient initially complained of shortness of breath on exertion. CXR revealed patchy infiltration in bilateral lower lobes which could be due to consolidation. There was no evidence of pneumothorax, pneumomediastinum, or subcutaneous emphysema then.

It was only on the 20th day of admission that she developed respiratory distress. The computed tomography of the chest revealed pneumomediastinum, massive subcutaneous emphysema, and bilateral pneumothoraces with collapse-

THE ASEAN JOURNAL OF RADIOLOGY
ISSN 2672-9393

consolidation of both lungs. The available literature reported that pneumomediastinum occurs mostly within 1 week of PQ ingestion [4,6,8]. However, there were 2 reported cases of pneumomediastinum that developed in the 2nd week while there were 2 cases of pneumothorax and 1 case of subcutaneous emphysema that developed after 2 weeks of PQ ingestion according to Im et al [6]. Therefore, that makes this a rare case scenario in which the patient developed pneumomediastinum after 2 weeks of PQ ingestion. Although one could argue that patients might have developed pneumomediastinum during the first 2 weeks as no follow-up CXR or CT was done then, those pneumomediastinums would have been small or insignificant as the patient was clinically stable without respiratory distress.

There are various theories explaining the pathogenesis of pneumomediastinum and pneumothorax. According to Im et al, it is caused by pulmonary interstitial emphysema with bullae formation when ruptures give rise to pneumothorax and subcutaneous emphysema [6]. Maunder et al postulated that it is probably caused by rupture of alveoli into bronchovascular sheath due to alveolar over-distension [9]. Another obvious cause would be esophageal perforation due to the caustic nature of PQ. In our patient, there was no evidence of esophageal perforation. However, there was air within bronchovascular sheath suggesting PQ-induced alveolar injury with subpleural bullae formation and subsequent rupture in accordance with Im et al. hypothesis.

Following the diagnosis, the patient was intubated, and bilateral ICD tubes were inserted. The patient expired the same day around the evening. This is in line with other literature which states that the presence of pneumomediastinum indicates poor prognosis [6,10]. The other poor prognostic CT findings include increased lung segment involvement, the extent of disease characteristics visualized in CT, and speed of progression from baseline [11].

Conclusion

Pneumomediastinum, pneumothorax and subcutaneous emphysema are rare subacute complications of paraquat poisoning and are associated with poor prognosis. Nevertheless, one needs to anticipate and recognize these complications for proper management.

References

1. Gunnell D, Eddleston M, Phillips MR, Konradsen F. The global distribution of fatal pesticide self-poisoning: systematic review. BMC Public Health 2007;7:357. doi: 10.1186/1471-2458-7-357.

2. National Plant Protection Centre. Department of Agriculture, Ministry of Agriculture & Forests [Internet]. Thimphu: NPPC; c2021 [cited 2021 Sept 1]. Herbicide 2016; [about 4 screens]. Available from: http://www.nppc.gov.bt/herbicide

3. Vale JA, Meredith TJ, Buckley BM. Paraquat poisoning: clinical features and immediate general management. Hum Toxicol 1987;6:41–7. doi: 10.1177/096032718700600107.

4. Chen KW, Wu MH, Huang JJ, Yu CY. Bilateral spontaneous pneumothoraces, pneumopericardium, pneumomediastinum, and subcutaneous emphysema: a rare presentation of paraquat intoxication. Ann Emerg Med 1994;23:1132–4. doi: 10.1016/s0196-0644(94)70116-4.

5. Delirrad M, Majidi M, Boushehri B. Clinical features and prognosis of paraquat poisoning: a review of 41 cases. Int J Clin Exp Med 2015;8:8122–8.

6. Im JG, Lee KS, Han MC, Kim SJ, Kim IO. Paraquat poisoning: findings on chest radiography and CT in 42 patients. AJR Am J Roentgenol 1991 ;157:697–701. doi: 10.2214/ajr.157.4.1892020.

7. Rose MS, Lock EA, Smith LL, Wyatt I. Paraquat accumulation: Tissue and species specificity. Biochemical Pharmacology 1976;25:419–23. doi: 10.1016/0006-2952(76)90344-0.

8. Daisley H, Barton EN. Spontaneous pneumothorax in acute paraquat toxicity. West Indian Med J 1990;39:180–5.

9. Maunder RJ, Pierson DJ, Hudson LD. Subcutaneous and mediastinal emphysema. Pathophysiology, diagnosis, and management. Arch Intern Med 1984;144: 1447–53.

10. Ackrill P, Hasleton PS, Ralston AJ. Oesophageal perforation due to paraquat. Br Med J 1978;1:1252–3. doi: 10.1136/bmj.1.6122.1252.

11. Zhang H, Liu P, Qiao P, Zhou J, Zhao Y, Xing X, et al. CT imaging as a prognostic indicator for patients with pulmonary injury from acute paraquat poisoning. Br J Radiol 2013;86:20130035. doi: 10.1259/bjr.20130035.

THE ASEAN JOURNAL OF RADIOLOGY
ISSN 2672-9393

Case Report

Spontaneous regression of the lung bulla

Rujaporn Daewa, M.D.
Pattharapong Saneha, M.D.
Laksika Bhuthathorn, M.D.
Natnicha Thetasen, M.D.
From Department of Radiology, Faculty of Medicine, Prince of Songkhla University, Songkhla, Thailand.
Address correspondence to R.D. (e-mail: rd.daewa@gmail.com)

Received 28 September 2021 ; revised 21 December 2021 ; accepted 24 December 2021
doi:10.46475/aseanjr.v22i3.154

Abstract

Blebs and bullae are gas-containing spaces commonly found in many conditions and usually cause no symptoms, but may progress over time resulting in respiratory distress; pneumothorax and superimpose infections are common complications of bullae. Spontaneous regression of the bulla is rarely encountered, and its mechanism remains unclear. However, a few case reports suggest that it usually occurs after an infection or a rupture.

We present a 72-year-old male ex-smoker who presented with progressive dyspnea for 1 month. His chest radiograph showed a few lung blebs and bullae in the right upper to middle lung field. Bronchodilators and anti-inflammatory medications were prescribed and he was referred to the pulmonologist. His first chest CT also showed multiple blebs and a large bulla in the bilateral upper lobes and he was scheduled for bullectomy because his bullae were symptomatic. However, at a 17-month follow up, his symptoms spontaneously improved and his chest CT showed regression of the bulla with only a few small calcifications and pleural thickening in the right upper lobe remaining.

Keywords: Bulla, Bleb, Regression, Spontaneous, Rupture.

Introduction

Blebs and bullae are gas-containing spaces commonly found in many conditions. Blebs are usually located within the visceral pleura or in the subpleural lung and are smaller than 1 cm in diameter while a bulla is described as a sharply demarcated region of emphysema larger than 1 cm in diameter with walls less than 1 mm thick [1].

Bullae usually cause no symptoms but may progress over time resulting in respiratory distress; pneumothorax and superimpose infections are common complications of bullae. Spontaneous regression of bulla is rarely found. Only 4 of 49 patients with decrease in size of bullous lesions during the x-ray follow up have been reported [2]. The mechanism in which this occurs remains unclear. A literature review and case report by Chang WH suggests that spontaneous regression of bullae usually occurs after an infection or a rupture [1].

Case summary

A 72-year-old male, 25-pack years ex-smoker who had quit for 5 years, presented with progressive dyspnea for 1 month. He complained of chest pain and dyspnea on exertion. The physical examination showed expiratory wheezing while the rest of his pulmonary and cardiovascular examination was unremarkable. His chest radiograph revealed multiple thin-walled lung lucencies, up to 6.1 cm in diameter, in the right upper to middle lung zone which was suspected to be bullae (Figure 1). Because of his history of chest pain on exertion, an electrocardiogram, cardiac enzyme test, as well as an echocardiogram were performed which found no abnormality. Bronchodilators were prescribed and he was sent to the pulmonologist.

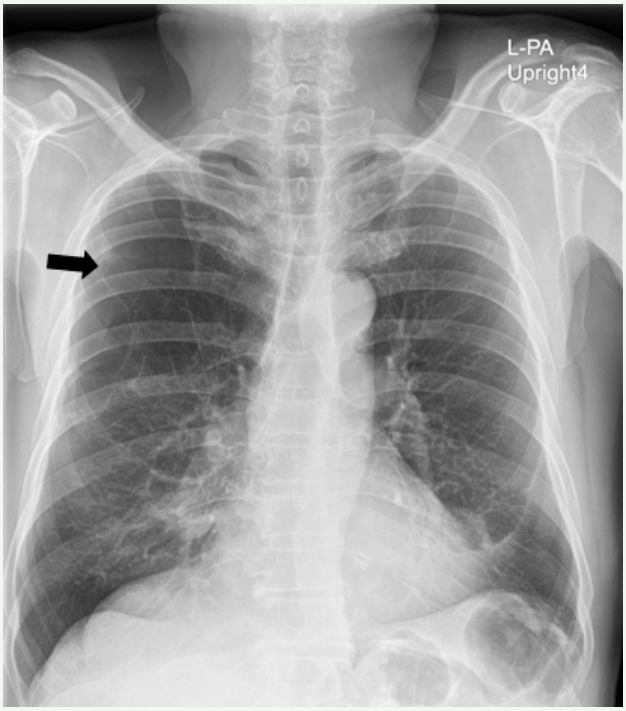

Figure 1. *Chest radiograph PA upright showed multiple lung blebs and bullae (black arrow) in the right upper to middle lung field.*

His pulmonary function test revealed an FEV1/FVC of 45% with an irreversible obstructive pattern and his postbronchodilator FEV1 was 75%; compatible with chronic obstructive pulmonary disease (COPD). He was treated with short and long-acting bronchodilators and inhaled corticosteroids. During a follow-up, his symptoms got worse. A chest CT was performed which revealed diffuse lung emphysema with multiple thin-walled blebs and bullae in the bilateral upper lobes (Figure 2A). He was discharged with bronchodilators and instructed to inhale corticosteroids and was scheduled for a bullectomy.

A few months later, he developed acute dyspnea with fever and was diagnosed with pneumonia at another local hospital where he received intravenous antibiotics for 3 days and was discharged once his symptoms improved. He then presented at our hospital for his follow-up chest CT (17 months after the previous study) which showed regression of the bullae with only a few residual small calcifications and pleural thickening in the right upper lobe observed (Figure 2B and 2C).

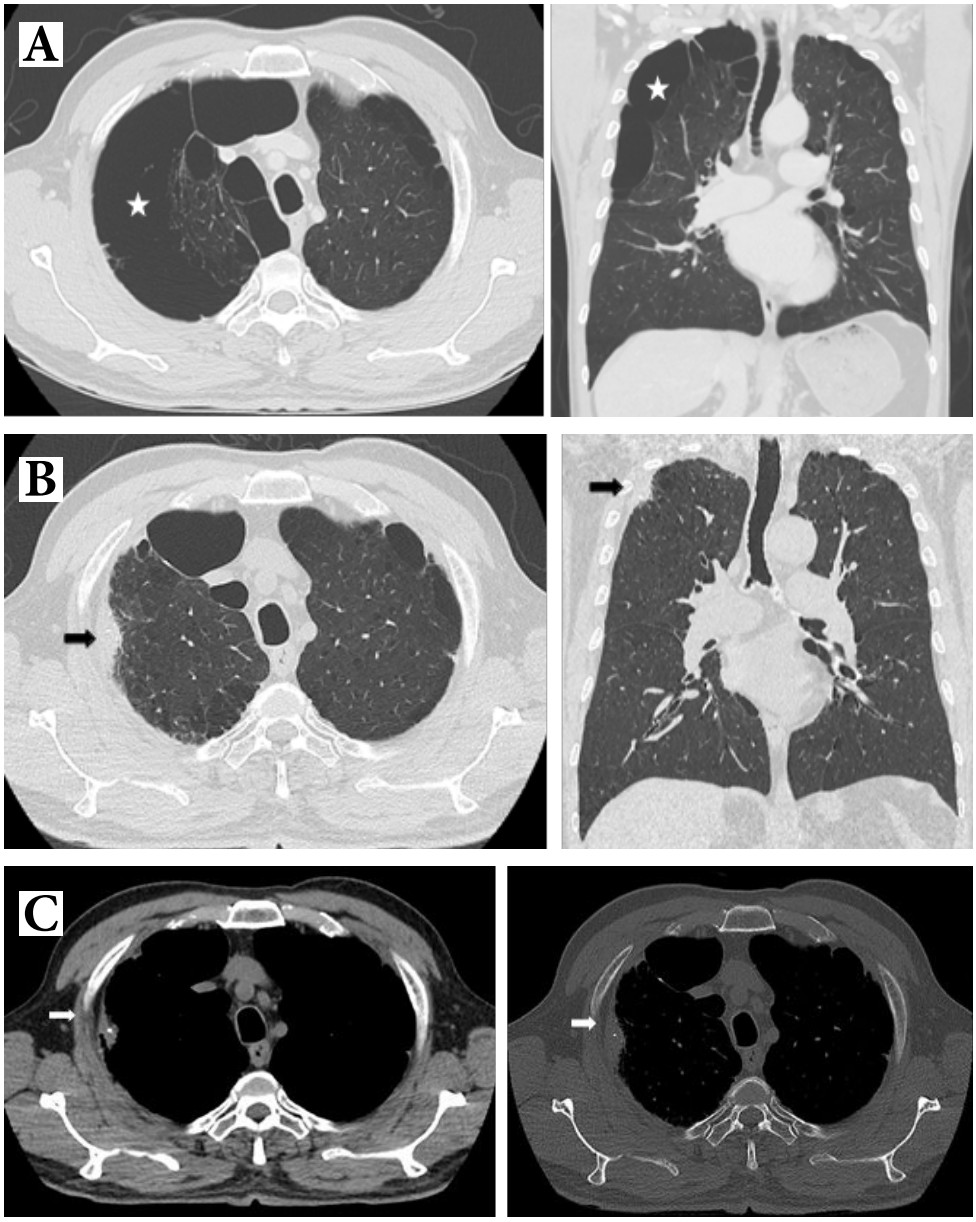

Figure 2. *Conventional chest CT in (A) lung window on axial and coronal views shows a few lung blebs (white stars) both upper lobes. 17 months later, his follow-up chest high resolution computed tomography (HRCT) in (B) lung window on axial and coronal views shows regression of the lung bullae (black arrows) in both upper lobes with new pleural thickening and a few small calcifications visualized in (C) axial mediastinum and bone window (white arrow) in right upper lobe.*

THE ASEAN JOURNAL OF RADIOLOGY
ISSN 2672-9393

Discussion

In the literature review by Chang [3], most cases of spontaneous regression of lung bullae occurred after an infectious process which could then result in inflammation of the airway and thus the closure of communication between the airway and bullae, converting the bullae into a closed space. The air within the closed-off bullae was then reabsorbed resulting in the disappearance of the bullae. Our patient reported a brief history of pulmonary infection before his follow-up chest CT which may precipitate the spontaneous regression of lung bullae in our case. However, no medical records and imaging evidence of his pulmonary infection was made available.

Chang [3] also suggested that smoking cessation and medical treatment could be associated with the regression of bullae. Tobacco smoke causes airway irritation and inflammation; smoking cessation combined with anti-inflammatory medication could decrease airway inflammation and relieve the check-valve obstruction of the airway, resulting in regression of bullae [3]. Our patient had a history of smoking cessation and also began continually receiving bronchodilators and anti-inflammatory medications after his first visit at our institution, prior to his initial chest CT. This seemed like the most probable explanation for the spontaneous regression of the bullae observed in our patient as his prior history of pulmonary infection remained questionable.

A few remaining small calcifications in the right upper lobe observed after the regression of bullae in our case also corresponded with the previous case report described by Benito Bernáldez et al [4]. However, no clear explanation about the pathophysiology of the calcification is described.

Despite the pathophysiology behind the spontaneous regression of the bullae remaining unclear, we suspect that bronchodilators and anti-inflammatory medications in conjunction with cessation of smoking may play a significant role in this particular case. Therefore, bronchodilator and anti-inflammatory medications with a close follow-up may be a good treatment option for patients with symptomatic bullae who refused surgical treatment, or in cases where bullectomy may not be a viable option due to surgical comorbidities.

References

1. Hansell DM, Bankier AA, MacMahon H, McLoud TC, Müller NL, Remy J. Fleischner Society: glossary of terms for thoracic imaging. Radiology 2008;246:697–722. doi: 10.1148/radiol.2462070712.

2. Boushy SF, Kohen R, Billig DM, Heiman MJ. Bullous emphysema: clinical, roentgenologic and physiologic study of 49 patients. Dis Chest 1968;54:327–34. doi: 10.1378/chest.54.4.327.

3. Chang WH. Complete spontaneous resolution of a giant bulla without rupture or infection: a case report and literature review. J Thorac Dis 2017;9:E551–5. doi: 10.21037/jtd.2017.05.53.

4. Benito Bernáldez C, Almadana Pacheco V. Spontaneous regression of pulmonary emphysematous bulla. Arch Bronconeumol 2017;53:347–8. doi: 10.1016/j.arbres.2016.09.001.

THE ASEAN JOURNAL OF RADIOLOGY
ISSN 2672-9393

ASEAN Movement in Radiology

Multidisciplinary working group for interstitial lung disease in Thailand: Part 1- rationale in developing a guide to estimate the global disease and fibrotic extents on high-resolution computed tomography

Wiwatana Tanomkiat, M.D.[(1)]
Chayanin Nitiwarangkul, M.D.[(2)]
Juntima Euathrongchit, M.D.[(3)]
Phakphoom Thiravit, M.D.[(4)]
Thanisa Tongbai, M.D.[(5)]
Thitiporn Suwatanapongched, M.D.[(2)]
From [(1)] Department of Radiology, Faculty of Medicine, Prince of Songkla University, Songkla, Thailand.
[(2)]Department of Diagnostic and Therapeutic Radiology, Faculty of Medicine Ramathibodi Hospital, Mahidol University, Bangkok, Thailand.
[(3)]Department of Radiology, Faculty of Medicine, Chiangmai University, Chiangmai, Thailand.
[(4)]Department of Radiology, Siriraj Hospital, Mahidol University, Bangkok, Thailand.
[(5)]Department of Radiology, Faculty of Medicine, Chulalongkorn University, Bangkok, Thailand.
Address correspondence to C.N. (email: chayanin.ntw@gmail.com)

Received 17 December 2021 ; accepted 19 December 2021
doi:10.46475/aseanjr.v22i3.158

Keywords: Interstitial lung disease, Fibrotic extent, Disease extent, Multidisciplinary discussion, Thailand.

Introduction

Interstitial lung diseases (ILDs) comprise a diverse group of diffuse lung parenchymal disorders, which are classified together due to similar clinical, radiologic, physiologic, or pathologic manifestations (Table 1) [1]. As shown in Table 1, most ILDs are caused by either known or unknown pathogens and are usually chronic. These include idiopathic interstitial pneumonias (IIPs; particularly idiopathic pulmonary fibrosis (IPF) and idiopathic nonspecific interstitial pneumonia (NSIP)), connective tissue disease-associated ILDs (CTD-ILDs), chronic hypersensitivity pneumonitis, familial pulmonary fibrosis, sarcoidosis, and other exposure-related diseases. Based on previous literature [2-5], the two most common ILDs in Western countries are idiopathic pulmonary fibrosis (IPF) and sarcoidosis, while the two most common ones in Asia are CTD-ILDs and IPF.

Table 1. *Clinical classification of diffuse lung parenchymal disorders [1].*

Idiopathic interstitial pneumonias (IIPs): idiopathic pulmonary fibrosis (IPF), idiopathic nonspecific interstitial pneumonia NSIP, cryptogenic organizing pneumonia (COP), respiratory bronchiolitis-interstitial lung disease (RB-ILD), desquamative interstitial pneumonia (DIP), lymphangitic carcinomatosis (LIP), acute interstitial pneumonia (AIP)
Connective tissue disease-associated ILDs (CTD-ILDs): rheumatoid arthritis (RA), systemic sclerosis (SSc), mixed connective tissue disease (MCTD), myositis, systemic lupus erythematosus (SLE), sjögren's syndrome
Eosinophilic lung disease: chronic eosinophilic pneumonia
Chronic lung disorders from drug reaction
Interstitial lung disease with granuloma: chronic granulomatous infections, sarcoidosis, hypersensitivity pneumonitis, berylliosis, etc.
Diffuse alveolar hemorrhage
Pneumoconiosis
Pulmonary hypertension and related disorder
Miscellaneous diseases: Langerhans cell histiocytosis, lymphangioleiomyomatosis, pulmonary alveolar proteinosis, amyloidosis, pulmonary alveolar microlithiasis, etc.
Malignant neoplasms: lymphangitic carcinomatosis, etc.

THE ASEAN JOURNAL OF RADIOLOGY
ISSN 2672-9393

ILDs can be suspected or diagnosed based on clinical and radiologic manifestations. The patients with ILD often present with dyspnea at rest or on exertion and has abnormal lung sounds on lung auscultation [6]. The two main physiologic changes on pulmonary function tests are restrictive pulmonary defect and decreased carbon monoxide diffusion capacity [7]. Chest radiography remains the most commonly performed primary imaging tool. However, the low sensitivity and specificity hinder its use [6]. Hence, high-resolution computed tomography (HRCT) has become a cornerstone for evaluating the morphology and distribution and diagnosing various ILDs [6].

At times, a confident diagnosis of several ILD entities can be made when patients have typical clinical and imaging findings, for example, usual interstitial pneumonia (UIP), lymphangitic carcinomatosis, lymphangioleiomyomatosis, Langerhans cell histiocytosis, pulmonary alveolar proteinosis, subacute hypersensitivity pneumonitis, asbestosis, and pulmonary edema [8]. The diagnosis of CTD-ILDs usually relies on clinical, physiologic, and radiologic data to define the presence of the disease, determine the clinical course, and assess the prognosis of the lung involvement [9].

Despite advances in knowledge, a significant proportion of ILDs remains complex and challenging to diagnose. Various ILDs often share common histological features and pathological mechanisms regardless of their causes. When the specific diagnosis cannot be entertained based on clinical, physiologic, and radiologic data, surgical lung biopsy (SLB), a gold standard tool for ILD diagnosis, may be required [10]. However, the procedure carries a high risk, especially in old or frail patients. The 30-day mortality is approximately 2.4% [11], comparable to the 2.3% 30-day mortality of lobectomy [12]. Hence, SLB is not a commonly performed procedure. As shown in previous studies, SLBs were performed in 1.8% in Indian National Registry [3], 8% in the previous study from a single center in Singapore [4], and less than 1% in the study from a single center in Southern Thailand [5].

Furthermore, SLBs are rarely performed in CTD-ILDs because there are no pathognomonic pathologic findings in CTD-ILDs, and the usefulness of a biopsy in predicting prognosis and management decisions is controversial. There is a tendency to treat all CTD patients with immunosuppressive therapies if they develop progressive clinical impairment or ILD on HRCT regardless of the histopathologic findings [8].

Due to inadequate pathologic data, a proportion ILDs remain unclassifiable because of insufficient data or significant discordance among the clinical, radiological or pathological findings. A specific diagnosis of ILD requires a multidisciplinary discussion (MDD), which has generally been accepted as the current diagnostic process for ILDs in many societies [13-15] since its introduction in 2004 [16]. The dynamic interaction and information exchange between physicians (pulmonologists and rheumatologists), radiologists, and pathologists help improve the diagnosis and management of ILD patients.

Progressive fibrosing interstitial lung disease (PF-ILD)

A proportion of ILD patients can have a progressive fibrosing clinical phenotype, termed progressive fibrosing interstitial lung disease (PF-ILD). PF-ILD is characterized by symptom worsening, a decline in lung function, and an increase to the extent of fibrosis on HRCT, which eventually leads to decreased quality of life and early death despite current therapy [17]. PF-ILD can also occur in patients with IPF, CTD-ILD, chronic hypersensitivity pneumonitis, familial pulmonary fibrosis, and unclassifiable ILDs.

Among IIPs, IPF is the most common and likely to have the worst prognosis [13,18]. Various studies [19-20], including a retrospective study from a single center in Southern Thailand [5], have reported that the survival time of patients with IPF was the shortest, while that of unclassifiable ILD cases was between that of the IPF and non-IPF patients. There is a guideline for the diagnosis and

THE ASEAN JOURNAL OF RADIOLOGY
ISSN 2672-9393

management of IPF providing levels of certainty for patterns of UIP based on HRCT and pathologic findings. The presence of the UIP pattern on HRCT in patients with clinically suspected IPF could guide a diagnosis if they are not subjected to SLB [10].

Previous studies [21-24] have found that antifibrotic therapies effectively slow down disease progression when lung fibrosis has become progressive. These included nintedanib and pirfenidone in IPF [21, 22] and nintedanib in systemic sclerosis-associated ILD (SSc-ILD) [23, 24]. In Thailand, nintedanib has been approved to treat patients with IPF diagnosed by MDD in 2016 and patients with SSc-ILD diagnosed by MDD, who has the fibrotic extent of more than 10% on HRCT and with PF-ILD feature in 2020. Moreover, the Thoracic Society of Thailand under Royal Patronage, the Thai Rheumatism Association, and the Thai Society of Pediatrics Respiratory and Critical Care Medicine recommend immunosuppressive therapies in SSc-ILD patients with the disease extent of more than 20% on HRCT.

A multidisciplinary working group in Thailand

At present, a clear definition of the ILD severity and fibrotic extent has become mandatory for the diagnosis, management, and treatment of patients with PF-ILDs. To facilitate communication among members and practitioners regarding the disease severity and fibrotic extent appearing on HRCT, the Royal College of Radiologists of Thailand and the Foundation for Orphan and Rare Lung Disease invited Thai thoracic radiologists and physicians (pulmonologists and rheumatologists) (Figure 1) to discuss the proposed method for estimation of ILD extent on December 3rd, 2021.

Figure 1. *Multidisciplinary working group on global disease and fibrotic extents on HRCT on December 3rd, 2021.*

Participant list:

1. Wiwatana Tanomkiat, M.D.	Songklanagarind Hospital, Prince of Songkla University
2. Sitang Nirattisaikul, M.D.	Songklanagarind Hospital, Prince of Songkla University
3. Nantaka Kiranantawat, M.D.	Songklanagarind Hospital, Prince of Songkla University
4. Thitiporn Suwatanapongched, M.D.	Ramathibodi Hospital, Mahidol University
5. Warawut Sukkasem, M.D.	Ramathibodi Hospital, Mahidol University
6. Chayanin Nitiwarangkul, M.D.	Ramathibodi Hospital, Mahidol University
7. Thanisa Tongbai, M.D.	King Chulalongkorn Memorial Hospital, Chulalongkorn University

8. Nitra Piyavisetpat, M.D.	King Chulalongkorn Memorial Hospital, Chulalongkorn University
9. Wariya Chintanapakdee, M.D.	King Chulalongkorn Memorial Hospital, Chulalongkorn University
10. Itthi Itthisawatpan, M.D.	King Chulalongkorn Memorial Hospital, Chulalongkorn University
11. Amornpun Wongkarnjana, M.D.	King Chulalongkorn Memorial Hospital, Chulalongkorn University
12. Juntima Euathrongchit, M.D.	Maharaj Nakorn Chiang Mai Hospital, Chiang Mai University
13. Yuttaphan Wannasopha, M.D.	Maharaj Nakorn Chiang Mai Hospital, Chiang Mai University
14. Phakphoom Thiravit, M.D.	Siriraj Hospital, Mahidol University
15. Suwimon Wonglaksanapimon, M.D.	Siriraj Hospital, Mahidol University
16. Pailin Ratanawatkul, M.D.	Srinagarind Hospital, Khon Kean University
17. Sumapa Chaiamnuay, M.D.	Phramongkutklao Hospital, Royal Thai Army Medical Department, Ministry of Defence
18. Krisna Dissaneevate, M.D.	Rajavithi Hospital, Department of Medical Services, Ministry of Public Health
19. Sutarat Tungsagunwattana, M.D.	Central Chest Institute of Thailand, Department of Medical Services, Ministry of Public Health
20. Sunpob Cheewadhanaraks, M.D.	Songklanagarind Hospital, Prince of Songkla University
21. Thunyarat Wiwattanapusit, M.D.	Songklanagarind Hospital, Prince of Songkla University
22. Natnicha Thet-asen, M.D.	Songklanagarind Hospital, Prince of Songkla University
23. Laksika Bhuthathorn, M.D.	Songklanagarind Hospital, Prince of Songkla University
24. Wethaka Kritcharoen, M.D.	Songklanagarind Hospital, Prince of Songkla University
25. Thitithep Suriyamonthon, M.D.	Songklanagarind Hospital, Prince of Songkla University

Our working group agreed that the ILDs should be estimated regarding all radiological features related to ILDs found on HRCT. These mainly include coarse reticulation, honeycombing, and traction bronchiectasis, considering the essential HRCT features of the UIP pattern since they are well correlated with fibrosis at histology and associated with increased mortality and poor prognosis [25-30]. Other CT findings suggesting non-ILD findings, such as cancer, pneumonia, or aspiration, are excluded from the estimation.

The extent of HRCT findings in each level can be determined by visually estimating the percentage to the nearest 5% parenchymal involvement. Minor interobserver variation or more reproducibility in estimation can be achieved by drawing a horizontal line on each level, leaving a measurable area of 50%, and then a second line, which runs perpendicularly to the horizontal one leaving a 25% assessable area of each lung. Each 25% is subdivided into five portions, corresponding to an area of 5% each [31] (Figure 2).

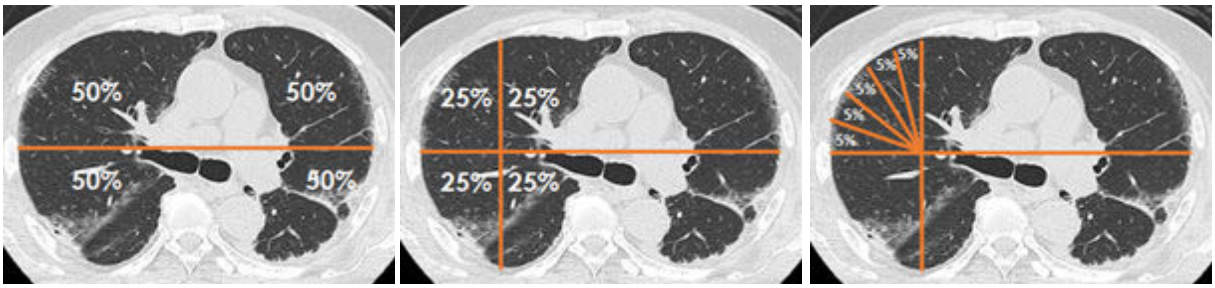

Figure 2. *Extent of disease assessment on HRCT using estimated to the nearest 5% method. This figure represents a cut of HRCT of a patient with SSc, at the level of the main carina. A drawing a horizontal line; leaving a measurable area of 50%, and then a second line, which runs perpendicularly to the horizontal line; leaving a 25% assessable area of each lung. Each 25% is subdivided into five portions, corresponding to an area of 5% each.*

Estimation of the global disease and fibrotic extents of ILD in both lungs can be quantified by averaging the summation of all three or five chosen HRCT levels previously described in the literature [29, 32]. The three-level method included the three selected HRCT levels from the upper, middle, and lower lung zones [32] (Figure 3). The five-level method included the HRCT levels at 1) the origin of

the great vessels; 2) the main carina; 3) the pulmonary venous confluence; 4) the halfway between levels 3 and 5; 5) immediately above the right hemidiaphragm dome [29]. However, the anatomical level defined in these methods, particularly the three-level method, is deemed unclear about which level to be assessed.

Estimation of ILD extent			
Level	Right lung (%)	Left lung (%)	Sum at each level (%)
Level 1 in upper zone	5%	10%	15%
Level 2 in middle zone	0%	5%	5%
Level 3 in lower zone	5%	5%	10%
Sum % (of all 3 levels or 6 areas)	30%		
Average extent (Sum% /6)	5%		

Figure 3. *Estimation of ILD extent.*
An example of a table demonstrates a calculation technique regarding the three-level method. Each side of HRCT level, the right and left lungs, was separately scored to the nearest 5%. The extent of disease (either global disease extent or fibrotic extent) is derived from the summation of all chosen HRCT levels divided by a number of areas of the lungs (total of 6 selected areas).

Noteworthy, many ILDs, especially IPF and SSc-ILD, are basal predominant. Moreover, patients with early ILD often have interstitial abnormalities confined to lung bases, specifically below the right hemidiaphragm dome. Hence, the global disease and fibrotic extent can be underestimated.

Since there are no clear description of how the level should be selected and the potentially inadequate inclusion of ILD extent, we have proposed the six-level method by modifying the original five-level method and adding level 6 (2-3 cm above the posterior costophrenic angle). The details regarding the six-level method will be further discussed in the upcoming article in the following journal issue. Nevertheless, the proposed method requires further validation to confirm its usefulness in evaluating ILDs in routine clinical practice. At present, the methods for estimating the ILD extent can still be based on personal preference.

References

1. Cosgrove GP, Schwarz MI. Approach to the evaluation and diagnosis of interstitial lung disease. In: Schwarz MI, King TE Jr., editors. Interstitial lung disease. 5th ed. Shelton (CT): People's Medical Pub. House; 2011. p. 3-33.

2. Rivera-Ortega P, Molina-Molina M. Interstitial lung diseases in developing countries. Ann Glob Health 2019;85:1-14. doi: 10.5334/aogh.2414.

3. Singh S, Collins BF, Sharma BB, Joshi JM, Talwar D, Katiyar S, et al. Interstitial lung disease in India: results of a prospective registry. Am J Respir Crit Care Med 2017;195:801-13. doi: 10.1164/rccm.201607-1484OC.

4. Chai GT, Tan TC, Lee YS, Kaw GJ, Chuah KL, Lim YJ, et al. Impact of an interstitial lung disease service in the diagnosis and management of interstitial lung disease in Singapore. Singapore Med J 2020;61:302-7. doi: 10.11622/smedj.2019069.

5. Tanomkiat W, Areewattana N, Juthong S, Navaskulpong A, Siripaitoon B, Sarayut LG. High-resolution computed tomography (HRCT) disease patterns and survival times in patients with interstitial lung disease at a university tertiary hospital in southern Thailand from 2006 to 2012. Asian J Med Radiol Res. Forthcoming 2022.

6. Wallis A, Spinks K. The diagnosis and management of interstitial lung diseases. BMJ 2015;350:h2072. doi: 10.1136/bmj.h2072.

7. Baydur A. Pulmonary physiology in interstitial lung disease: recent developments in diagnostic and prognostic implications. Curr Opin Pulm Med 1996;2:370-5. doi: 10.1097/00063198-199609000-00005.

8. Lynch DA. Radiologic differential diagnosis of diffuse lung disease. In: Lynch DA , Newell DJ Jr, Lee JS, editors. Imaging of diffuse lung disease. Hamilton (Ontario): B.C. Decker; 2000: p. 35-56.

9. Mira-Avendano I, Abril A, Burger CD, Dellaripa PF, Fischer A, Gotway MB, et al. Interstitial lung disease and other pulmonary manifestations in connective tissue diseases. Mayo Clin Proc 2019;94:309-25. doi: 10.1016/j.mayocp.2018.09.002.

10. Raghu G, Remy-Jardin M, Myers JL, Richeldi L, Ryerson CJ, Lederer DJ, et al. Diagnosis of idiopathic pulmonary fibrosis. an official ATS/ERS/JRS/ALAT clinical practice guideline. Am J Respir Crit Care Med 2018;198:e44-68. doi: 10.1164/rccm.201807-1255ST.

11. Hutchinson JP, McKeever TM, Fogarty AW, Navaratnam V, Hubbard RB. Surgical lung biopsy for the diagnosis of interstitial lung disease in England: 1997-2008. Eur Respir J 2016;48:1453-61. doi: 10.1183/13993003.00378-2016.

12. Powell HA, Tata LJ, Baldwin DR, Stanley RA, Khakwani A, Hubbard RB. Early mortality after surgical resection for lung cancer: an analysis of the English National Lung cancer audit. Thorax 2013;68:826-34. doi: 10.1136/thoraxjnl-2012-203123.

13. Travis WD, Costabel U, Hansell DM, King TE Jr, Lynch DA, Nicholson AG, et al. An official American Thoracic Society/European Respiratory Society statement: update of the international multidisciplinary classification of interstitial pneumonias. Am J Respir Crit Care Med 2013;188:733–48. doi: 10.1164/rccm.201308-1483ST.

14. Lynch DA, Sverzellati N, Travis WD, Brown KK, Colby TV, Galvin JR, et al. Diagnostic criteria for idiopathic pulmonary fibrosis: a Fleischner Society White Paper. Lancet Respir Med 2018;6:138–53. doi: 10.1016/S2213-2600(17)30433-2.

15. Prasad JD, Mahar A, Bleasel J, Ellis SJ, Chambers DC, Lake F, et al. The interstitial lung disease multidisciplinary meeting: a position statement from the Thoracic Society of Australia and New Zealand and the Lung Foundation Australia. Respirology 2017;22:1459–72. doi: 10.1111/resp.13163.

16. Flaherty KR, King TE Jr, Raghu G, Lynch JP 3rd, Colby TV, Travis WD, et al. Idiopathic interstitial pneumonia: what is the effect of a multidisciplinary approach to diagnosis? Am J Respir Crit Care Med 2004;170:904-10. doi: 10.1164/rccm.200402-147OC.

17. Wijsenbeek M, Kreuter M, Olson A, Fischer A, Bendstrup E, Wells CD, et al. Progressive fibrosing interstitial lung diseases: current practice in diagnosis and management. Curr Med Res Opin 2019;35:2015-24. doi: 10.1080/03007995.2019.1647040.

18. Kim DS, Collard HR, King TE Jr. Classification and natural history of the idiopathic interstitial pneumonias. Proc Am Thorac Soc 2006;3:285-92. doi: 10.1513/pats.200601-005TK.

19. Ryerson CJ, Urbania TH, Richeldi L, Mooney JJ, Lee JS, Jones KD, et al. Prevalence and prognosis of unclassifiable interstitial lung disease. Eur Respir J 2013;42:750-7. doi: 10.1183/09031936.00131912.

20. Traila D, Oancea C, Tudorache E, Mladinescu OF, Timar B, Tudorache V. Clinical profile of unclassifiable interstitial lung disease: comparison with chronic fibrosing idiopathic interstitial pneumonias. J Int Med Res 2018;46:448-56. doi: 10.1177/0300060517719767.

21. King TE Jr, Bradford WZ, Castro-Bernardini S, Fagan EA, Glaspole I, Glassberg MK, et al. A phase 3 trial of pirfenidone in patients with idiopathic pulmonary fibrosis. N Engl J Med 2014;370:2083-92. doi: 10.1056/NEJMoa1402582.

22. Richeldi L, du Bois RM, Raghu G, Azuma A, Brown KK, Costabel U, et al. Efficacy and safety of nintedanib in idiopathic pulmonary fibrosis. N Engl J Med 2014;370:2071-82. doi: 10.1056/NEJMoa1402584.

23. Distler O, Highland KB, Gahlemann M, Azuma A, Fischer A, Mayes MD, et al. Nintedanib for systemic sclerosis–associated interstitial lung disease. N Engl J Med 2019;380:2518-28. doi: 10.1056/NEJMoa1903076.

24. Wells AU, Flaherty KR, Brown KK, Inoue Y, Devaraj A, Richeldi L, et al. Nintedanib in patients with progressive fibrosing interstitial lung diseases -subgroup analyses by interstitial lung disease diagnosis in the INBUILD trial: a randomised, double-blind, placebo-controlled, parallel-group trial. Lancet Respir Med 2020;8: 453-60. doi: 10.1016/S2213-2600(20)30036-9.

25. Ryerson CJ, Vittinghoff E, Ley B, Lee JS, Mooney JJ, Jones KD, et al. Predicting survival across chronic interstitial lung disease: the ILD-GAP model. Chest 2014;145:723–8. doi: 10.1378/chest.13-1474.

26. Flaherty KR, Thwaite EL, Kazerooni EA, Gross BH, Toews GB, Colby TV, et al. Radiological versus histological diagnosis in UIP and NSIP: survival implications. Thorax 2003;58:143–8. doi: 10.1136/thorax.58.2.143.

27. Kim EJ, Elicker BM, Maldonado F, Webb WR, Ryu JH, Van Uden JH, et al. Usual interstitial pneumonia in rheumatoid arthritis-associated interstitial lung disease. Eur Respir J 2010;35:1322–28. doi: 10.1183/09031936.00092309.

28. Oldham JM, Adegunsoye A, Valenzi E, Lee C, Witt L, Chen L, et al. Characterisation of patients with interstitial pneumonia with autoimmune features. Eur Respir J 2016;47:1767–75. doi: 10.1183/13993003.01565-2015.

29. Goh NS, Desai SR, Veeraraghavan S, Hansell DM, Copley SJ, Maher TM, et al. Interstitial lung disease in systemic sclerosis: a simple staging system. Am J Respir Crit Care Med 2008;177:1248-54. doi: 10.1164/rccm.200706-877OC.

30. Morisset J, Vittinghoff E, Lee BY, Tonelli R, Hu X, Elicker BM, et al. The performance of the GAP model in patients with rheumatoid arthritis associated interstitial lung disease. Respir Med 2017;127:51-6. doi: 10.1016/j.rmed.2017.04.012.

31. Sánchez RP, Fernández-Fabrellas E, Samper GJ, Montañana MLD, Vilar LN. Visual HRCT score to determine severity and prognosis of idiopathic pulmonary fibrosis. Int J Respir Pulm Med 2018;5:084. doi.org/10.23937/2378-3516/1410084.

32. Kazerooni EA, Martinez FJ, Flint A, Jamadar DA, Gross BH, Spizarny DL, et al. Thin-section CT obtained at I 0-mm increments versus limited three-level thin-section CT for idiopathic pulmonary fibrosis: correlation with pathologic scoring. AJR Am J Roentgenol 1997;169:977-83. doi: 10.2214/ajr.169.4.9308447.

ASEAN

This journal provide 4 areas of editorial services: language editing, statistical editing, content editing, and complete reference-citation check in 8 steps:

Step	Services to authors	Services providers
I	Manuscript submitted	Editor
II	Language editing/ A reference-citation check	Language consultant/Bibliographer
III	First revision to ensure that all information remains correct after language editing	Editor
IV	Statistical editing	Statistical consultant
V	Content editing*	Two reviewers
VI	Second revision	Editor
VII	Manuscript accepted/ rejected	Editor/Editorial board
VIII	Manuscript published	Editorial office

*Content editing follows a double-blind reviewing procedure

JOURNAL OF RADIOLOGY